

HELENE GRØTTING & TRUDE MORK

SUPERVISOR: MALCOLM A. KELLAND



Universitetet
i Stavanger

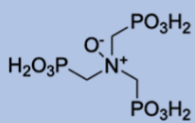
Scale Inhibitors for Water Treatment

Master's Thesis 2024

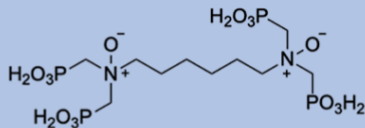
Environmental Engineering

Department of Chemistry, Bioscience and Environmental Engineering

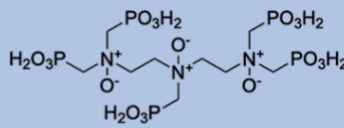
Faculty of Science and Technology



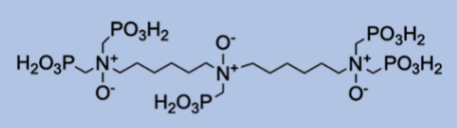
ATMP-O



HMDTP-O



DTPMP-O



BHMPMPA-O



1. Abstract

Scale formation is a common water-based challenge in the oil and gas industry, alongside gas hydrates and corrosion. It accumulates on pipelines and wellbores, reducing flow rates and damaging downhole equipment, resulting in loss of production efficiency. The primary method for minimizing scale formation in this sector is by using scale inhibitors (SI). These inhibitors work by delaying or preventing the formation of scale. Aminophosphonates are commonly used as SIs in the oil and gas industry due to their excellent metal binding capacity and high thermostability, making them particularly useful in SI squeeze treatments. However, a significant challenge with many aminophosphonate inhibitors is their limited compatibility with calcium ions. It often results in the precipitation of calcium complexes, reducing their efficiency.

This study aims to modify existing aminophosphonates by oxidizing them to aminophosphonate oxides to increase their hydrophilicity, improve their calcium compatibility and potentially improve their performance. Additionally, we aim to determine whether the aminophosphonate oxides exhibit better or worse thermal stability compared to aminophosphonates after undergoing anaerobic thermal aging.

Four commercial SIs—Amino-tris(methylenephosphonic acid) (ATMP), hexamethylenediamine tetra(methylenephosphonic acid) (HMDTP), diethylenetriamine penta(methylphosphonic) acid (DTPMP) and bis(hexamethylene triaminepenta(methylene-phosphonic acid) (BHMTMPMPA)—were oxidized using hydrogen peroxide. The efficiency of the oxides and their commercial forms was tested on a high-pressure dynamic tube blocking scale rig at 100 °C and 80 bars at various SI concentrations against calcium carbonate and barium sulfate scale. Additionally, all SIs underwent calcium compatibility testing to examine the rate and occurrence of SI-calcium complex precipitation and thermal aging testing to evaluate their stability for downhole squeeze treatments in oilfield wells.

In general, all inhibitors demonstrated effective inhibition properties against calcite scale at pH 6, though there was a slight decrease in effectiveness after oxidation. The same was seen against barite scale, however, larger inhibitor molecules exhibit better inhibition properties than smaller molecules. Calcium compatibility tests show little or no improvement after oxidation, but results indicated that SIs with longer carbon backbones were more compatible with calcium ions than those with shorter carbon backbones. Considering both

calcite and barite scales, HMDTP, BHMTMPMA and their oxides exhibited the best stability in thermal aging tests.

In conclusion, among the oxides, HMDTP-O proved to be effective at lower concentrations and demonstrated the most improvements in calcium compatibility and great thermal stability. However, BHMTMPMA also showed some of the same advantages, so a thorough evaluation of the pros and cons is necessary.

2. Acknowledgement

We would like to thank Professor Malcolm A. Kelland for all his help and support during the completion of our master's thesis in Environmental Engineering at the University of Stavanger in June 2024. We are grateful for the opportunity to be a part of his research group, and this academic journey would not have been possible without his assistance.

Additionally, we want to thank each other for our collaborative efforts during the practical work. The practical lab work was performed at Professor Kelland's chemistry laboratory at UiS from January 2024 – May 2024. Our mutual commitment and teamwork were necessary in completing this research.

We would also like to express our sincere thanks to Maryam Tahlil Warsame and Abdelrahman Abdelaal for their essential training in operating the scale rig. Their assistance and support throughout this research process have been important, and we are very grateful for their continuous help and collaboration.

Finally, thank you to our friends and family who have supported us during our academic journey. Your encouragement has been important, and this achievement would not have been possible without your support.

Helene Grøtting & Trude Mork

Table of Contents

1. Abstract	I
2. Acknowledgement	III
Abbreviations	VI
3. Introduction	1
3.1. Background	1
3.2. Types of Scale	3
3.2.1. Calcium Carbonate Scale	4
3.2.2. Sulfate Scale	5
3.2.3. Sulfide Scale	5
3.2.4. Sodium Chloride Scale	6
3.2.5. Mixed Scale	6
3.3. Scale Formation	7
3.3.1. Mechanism	7
3.3.2. Thermodynamic and Kinetics in Prediction of Scale Formation	11
3.4. Scale Inhibitors	13
3.4.1. Mechanism	14
3.4.2. Phosphonates and Aminophosphonates as Scale Inhibitors	15
3.5. Application of Scale Inhibitors	19
3.5.1. Batch Treatment	20
3.5.2. Continuous Injection	20
3.5.3. Squeeze Treatment	21
4. Experimental	25
4.1. Chemicals and Equipment	25
4.2. Synthesis	25
4.2.1. pH Adjustment	27
4.3. Characterization of SIs	27
4.4. High-Pressure Dynamic Tube Blocking Test Protocol	28
4.4.1. Problems with High-Pressure Dynamic Tube Blocking Scale Rig	31
4.5. Calcium Compatibility Test	32
4.6. Thermal Stability Test	33
5. Results and Discussion	34

5.1.	High-Pressure Dynamic Tube Blocking Test.....	34
5.1.1.	pH 6.....	34
5.1.2.	Various pH Levels.....	39
5.2.	Calcium Compatibility Test	42
5.3.	Thermal Stability Test.....	44
6.	Conclusion	47
	References	49
	Appendix	57
A-1	NMR Spectra.....	57
A-2	High-Pressure Dynamic Tube Blocking Rig Test Results	66
A-3	Calcium Compatibility Test Results.....	68

Abbreviations

SI	Scale Inhibitor
MIC	Minimum Inhibitor Concentration
SRB	Sulfate Reducing Bacteria
K _{sp}	Solubility Product Constant
OSPAR	Oslo and Paris Commission
NMR	Nuclear Magnetic Resonance
ATMP	Amino-tris (methylenephosphonic acid)
ATMP-O	Amino-tris (methylenephosphonic acid) oxide
HMDTP	Hexamethylenediamine tetra(methylenephosphonic acid)
HMDTP-O	Hexamethylenediamine tetra(methylenephosphonic acid) oxide
DTPMP	Diethylenetriamine penta(methylphosphonic) acid
DTPMP-O	Diethylenetriamine penta(methylphosphonic) acid oxide
BHMTMPMPA	Bis(hexamethylene triaminepenta(methylenephosphonic acid))
BHMTMPMPA-O	Bis(hexamethylene triaminepenta(methylenephosphonic acid) oxide)
EDTA	Ethylenediaminetetraacetic acid
FIC	Failed Inhibitor Concentration

3. Introduction

3.1. Background

Scale formation is a frequent challenge that significantly influences the production and transportation of hydrocarbons in the oil and gas sector. It is likely one of the primary problems associated with water-related production, alongside gas hydrates and corrosion. Formation of scale occurs when inorganic salts with limited solubility are deposited from water-based solutions [1]. In oilfields, scale is formed by the precipitation of hard mineral compounds from brine solution when temperature and pressure changes [2], [3]. Scale has the capability to adhere to nearly any surface, and without treatment, it will continuously increase in thickness [4]. This provides a range of different challenges. It can form anywhere along the production pipe, decreasing the internal diameter [1]. The build-up of scale on pipelines and wellbores can lead to reduced flow rates and damaged downhole equipment, affecting production effectiveness, and resulting in substantial economic losses [2], [3].

The most common scale deposition products in oilfields are calcium carbonate and calcium, barium and strontium sulfate [5]. A variety of variables including pH, pressure, temperature, solution saturation, the flow hydrodynamic behavior, concentration/dilution and partial pressure of CO₂ influence the formation of scale [6], [7]. The different scale deposits can also be categorized as either “pH-independent” or “pH-sensitive”. The sulfates are classified as pH independent as the brine’s pH does not majorly affect the scaling tendency. Carbonates are soluble in acid, and the pH of the brine has a significant impact on their scaling tendencies. The carbonates are therefore categorized as pH-sensitive [5].

The most popular method for controlling scale formation in the oil and gas industry is chemical treatment with scale inhibitors (SIs). These are low-dosage, water-soluble chemicals that are designed to inhibit crystal growth, nucleation, and precipitation of scales in oil and gas wells during production [8]. This is called a threshold SI treatment and works by interfering with one or more of the stages of scale formation to stop or delay the deposition [9]. To achieve a specific level of scale inhibition, the concentration must exceed a certain threshold level, which is called minimum inhibitor concentration (MIC) [10]. By covering the scale that has developed in the aggregate, the SI functions as a nucleation center. As a result, active crystal growth sites are inhibited which prevents additional crystal

growth [9]. When applied either by continual injection or by squeeze treatment into the near wellbore formation, chemical inhibitors have been generally considered the most cost-effective solution to prevent scale formation and contribute to benefits like reducing freshwater consumption, recovery of thermal energy, and cost savings associated with periodic pipeline cleaning [2], [11].

The economic consequences of scales and organic deposits cost billions of dollars annually, and inorganic scale-related damages, excluding corrosion, are estimated at around \$2 billion per year [1], [12]. The emergence of various issues coming from inorganic scales and mixed organic deposits is unavoidable as reservoirs age globally.

3.2. Types of Scale

The main cause of scale formation is the incompatibility of anions and cations in water [13]. During the production process in oil and gas fields, massive volumes of water containing significant levels of dissolved salts are generated and managed. A mix of these waters leads to supersaturated solutions, which gives deposition of scale. Scales are also formed due to changes in temperature and pressure of the produced water, leading to disturbance of the thermodynamic equilibrium [14]. Decreasing temperature and pressure results in decreased solubility for most minerals. Calcium carbonate is an exception, where decreasing temperature gives an increased solubility [15]. Figure 3.1 shows an example of barium sulfate in a production pipe [16].

The predominant inorganic scales in the oil industry, listed in order of frequency, include [1]:

- Calcium carbonate
- Sulfate salts of calcium, barium and strontium
- Sulfide scales of iron (II), lead (II) and zinc
- Sodium chloride

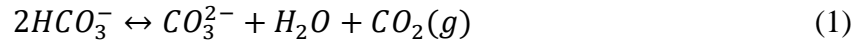


Figure 3.1 Barium sulfate scale in production pipe [16].

3.2.1. Calcium Carbonate Scale

Calcium carbonate (CaCO_3) is the most prevalent type among carbonate scales [17]. At reservoir conditions, calcite emerges as the most stable form of CaCO_3 scale. The tendencies of carbonate scale formation are affected by varying sets of hydrodynamic, kinetic and thermodynamic conditions when brine, oil and gas are mixed in the reservoirs or wellbores [7], [18].

Calcium ions (Ca^+) and bicarbonate ions (HCO_3^-) are normally present in formation waters. The transformation of bicarbonate into carbonate is achieved through equilibrium 1. If the pressure of the system decreases, the equilibrium shifts to the right, aiming to elevate the pressure by forming additional CO_2 (g), due to Le Chatelier's principle. This leads to an increased formation of carbonate ions, which rises the pH [1], [19].



The precipitation of calcium carbonate, shown in reaction 2, occurs when the concentration of carbonate reaches a sufficiently high level.



Higher temperatures result in a lower CaCO_3 solubility meaning it reduces the equilibrium constant for the dissolution of calcium carbonate, favoring the precipitation of solid calcium carbonate. It is therefore expected that CaCO_3 scales appear in geothermal systems, and care should be taken when operating wells at temperatures greater than 100 °C [20]. The precipitation of calcium carbonate scale is also significantly influenced by the pH of the water. Bicarbonate ions dominate the water at lower pH levels. As pH increases, carbonate ions become more prevalent and available to react with Ca^{2+} ions to form the calcium carbonate scale. Usually, the calcium carbonate scale is formed in the upper parts of completions [21], [22].

3.2.2. Sulfate Scale

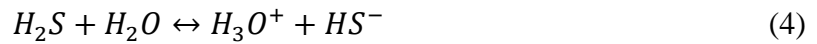
Sulfate scale commonly occurs when two or more incompatible waters like formation water and injected seawater are mixed [1], [23], [24]. The injection of seawater into the formation reservoir is a common practice aimed at enhancing oil recovery rates. However, this can lead to significant scaling problems in both the downhole formation and at the bottom of the wellfield [25], [26]. Sulfate ions can produce a sparingly soluble scale when mixed with metal ions from Group II, except magnesium. As you go down the group of metals, the solubility of sulfates decreases. The following equation shows the general reaction [1]:



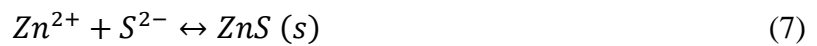
Barium sulfate (BaSO₄) is the most insoluble scale that can develop in oilfield waters, which leads to the formation of a hard scale that is difficult to remove [24]. The solubility product of BaSO₄ increases as the temperature, pressure, and the brine's salt concentration rise [24], [27]. Because of this, in high-pressure, high-temperature reservoirs with long residence time, production wells face the risk of barium sulfate scale deposition near the wellbore or within the tubing [27]. When there is a high risk of barium sulfate scale deposition for a specific site, it is highly recommended to prevent scale formation, as it is challenging to remove once it forms.

3.2.3. Sulfide Scale

Compared to carbonate and sulfate scales, sulfide scales are less frequent. However, it can still cause significant problems if left uncontrolled. This scale is primarily formed through the interaction of hydrogen sulfide with iron, zinc or lead. Iron ions mainly result from the corrosion of steel, occurring in either the injector or producing well, while zinc and lead ions are present in some formation waters. In oil wells, the majority of hydrogen sulfide results from the activity of sulfate-reducing bacteria (SRBs) acting on sulfate ions in the injected seawater. Sulfate ions are reduced by these SRBs to hydrogen sulfide (H₂S), which is in equilibrium with hydrosulfide and sulfide ions [1]:



The three mentioned sulfide scales are formed by the following equations:



3.2.4. Sodium Chloride Scale

Sodium chloride has a significantly higher solubility compared to the scales described previously. Its solubility also tends to increase with rising temperature. This salt may be found in very high quantities in some formation waters, especially in reservoirs under high pressure and temperature. As a result, the formation water can be saturated in sodium chloride. Sodium chloride may precipitate out of the produced water as its temperature drops. If this process is left untreated, a conduit may block quickly due to the fast kinetics [1].

3.2.5. Mixed Scale

Under certain conditions, scales can occur as layers of different types, such as both sulfate and carbonate scales. These formations can be oily and can also contain asphaltene deposits. This is known as soft scale, and it makes the chemical remediation process more complicated [1].

3.3. Scale Formation

3.3.1. Mechanism

Scale formation occurs when one or more sparingly soluble salts become supersaturated due to process conditions. When the solution is supersaturated, crystallization or precipitation becomes thermodynamically possible. The crystallization process consists of four main stages [28]:

- Aggregation
- Nucleation
- Crystal growth around the nucleus
- Agglomeration

Aggregation occurs when the water becomes supersaturated with scaling ions, which leads to collisions between cationic and anionic species, forming ion pairs in the solution. These ion pairs then turn into micro-aggregates, and work as nucleation centers for crystallization. These micro-crystals then grow into larger ones before they fuse together to form adherent macro-crystals during the crystal growth stage. The agglomeration stage is characterized by the growth of macro-crystals into a scale film on a surface. This eventually results in scale deposit through adsorption of more scaling ions from the solution [29]. The steps of the formation process are illustrated in Figure 3.2.

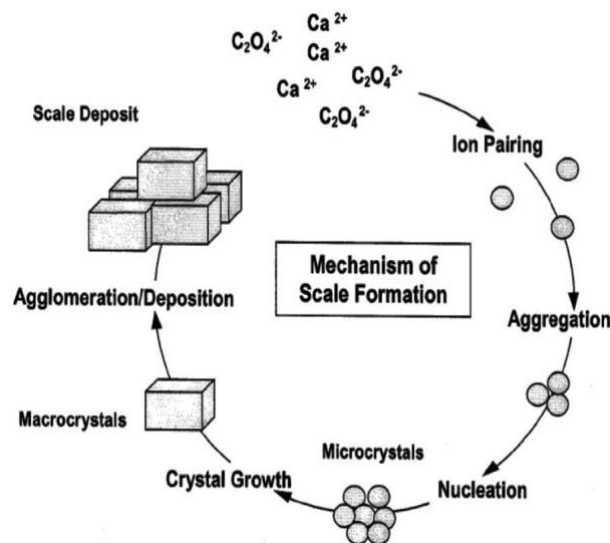


Figure 3.2 Schematic illustration of the scale formation mechanism pathway with calcium carbonate scale as an example [30].

There are two crystallization processes known to cause scale formation: bulk crystallization and surface crystallization [28], [31]. Bulk crystallization occurs when crystal particles form in the bulk phase through homogeneous crystallization. The supersaturated brine causes scale-forming ions to aggregate through random collisions while in motion. These ion clusters merge to form crystals, and once they exceed a critical size, precipitation takes place [32]. These particles can then settle on pipe surfaces as sediments or particles, resulting in flux decline as they form a cake layer. Surface crystallization occurs as a result of the lateral growth of the scale deposit, leading to reduced flux and blockage of the surface. Figure 3.3 illustrates the two crystallization processes schematically [33].

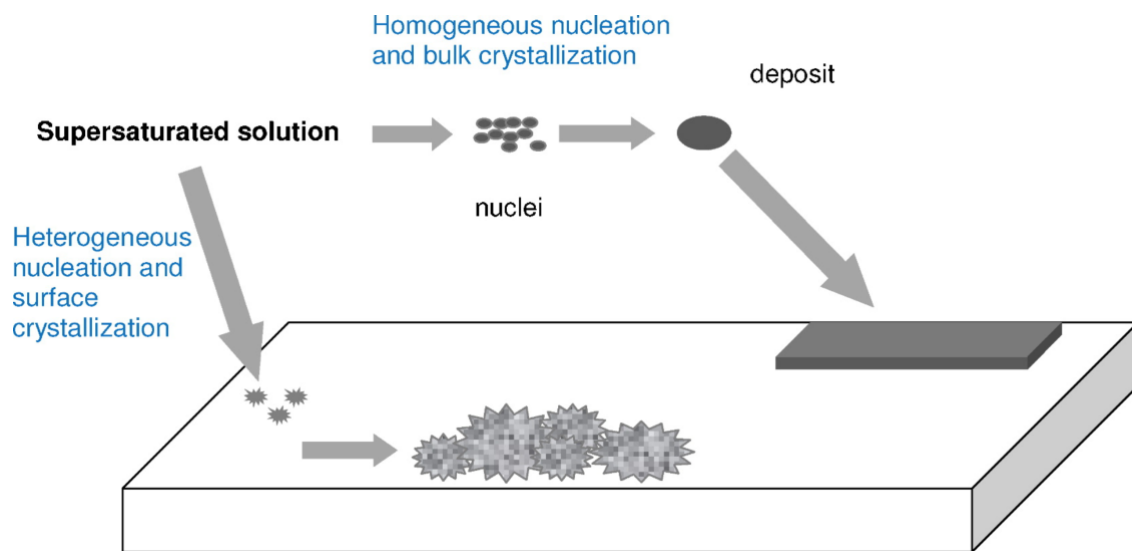


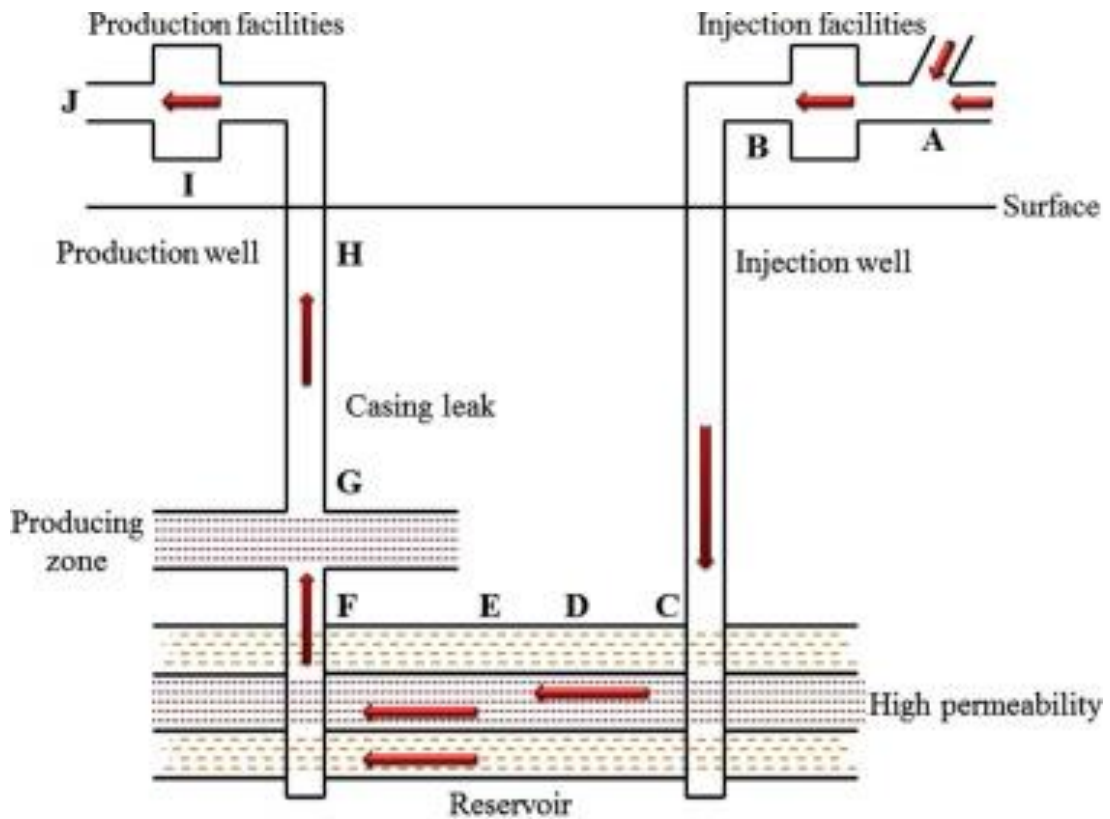
Figure 3.3 Illustration of bulk crystallization and surface crystallization [33].

Both mechanisms contribute to scaling formation in a pipe system and are affected by the system's process conditions. Additionally, under supersaturated scale-forming conditions, scale growth and agglomeration occur [28]. Scale formation in oil and gas fields can also be affected by a variety of operational parameters like temperature, pH, flow velocity, permeation rate, operating pressure, and the presence of metal ions or other salts. The primary cause of scale formation is the incompatibility between cations and anions in water [13].

The precipitation and crystallization kinetics should also be considered as it is an essential factor in the degree of scaling [32]. When the critical value for supersaturation is crossed, crystals will grow due to nucleation of scale formation of particle surfaces. Temperature, pH, flow velocity, operating pressure, the types of pre-treatments and the presence of other metal ions are parameters that have been reported to influence the scale formation kinetics [32]. A low concentration of nucleation sites will also affect the crystallization kinetics by slowing it down [13], [33], [34].

Because scales are impermeable by nature, they often build up on solid surfaces. As surface roughness rises, so does the tendency of scale deposition. As soon as the deposition begins, it gets easier to deposit the next layer, and over time, more and more layers of scale accumulate on the surface. Surface features like separators and heater treaters, as well as the interior surface of pipelines, chokes, subterranean pumps, and other equipment, are prime candidates for scale deposition in an oil well [10]. The outcome may lead to failures in production equipment, emergency shutdowns, heightened maintenance expenses, and a general decline in production efficiency. In water injection systems, the scale could block the formation pores, leading to a gradual decrease in injection rate over time [35].

The various conditions contributing to the production of scale at different sites during water flooding are illustrated in Figure 3.4.



Location	Changes which could produce scale formation
A to B	Mixing of brines for injection.
B to C	Pressure and temperature increase.
C to D	Pressure decline and continued temperature increase.
C to F	Solution composition may be adjusted by cation exchange, mineral dissolution or other reactions with rock.
D to F	Mixing of brines in the reservoir.
E to J	Pressure and temperature decline. Release of carbon dioxide and evaporation of water due to the pressure decline if a gas phase is present or forms between these locations.
F	Mixing of formation water and injection water which has "broken through" at the base of the production well.
G	Mixing of brines produced from different zones.
H	Mixing of produced brine with brine from casing leak.

Figure 3.4 Schematic illustration of scale formation in an oilfield undergoing water flooding [36].

3.3.2. Thermodynamic and Kinetics in Prediction of Scale Formation

A major component in scale management is the prediction of the scaling tendency of a production system [37]. Thermodynamics and kinetics give insights into the possibility and rate of scaling reactions. While thermodynamics focuses on equilibrium conditions, kinetics describes reaction rates, determined by activation energy thresholds [10]. Figure 3.5 illustrates the energy progress of a reaction.

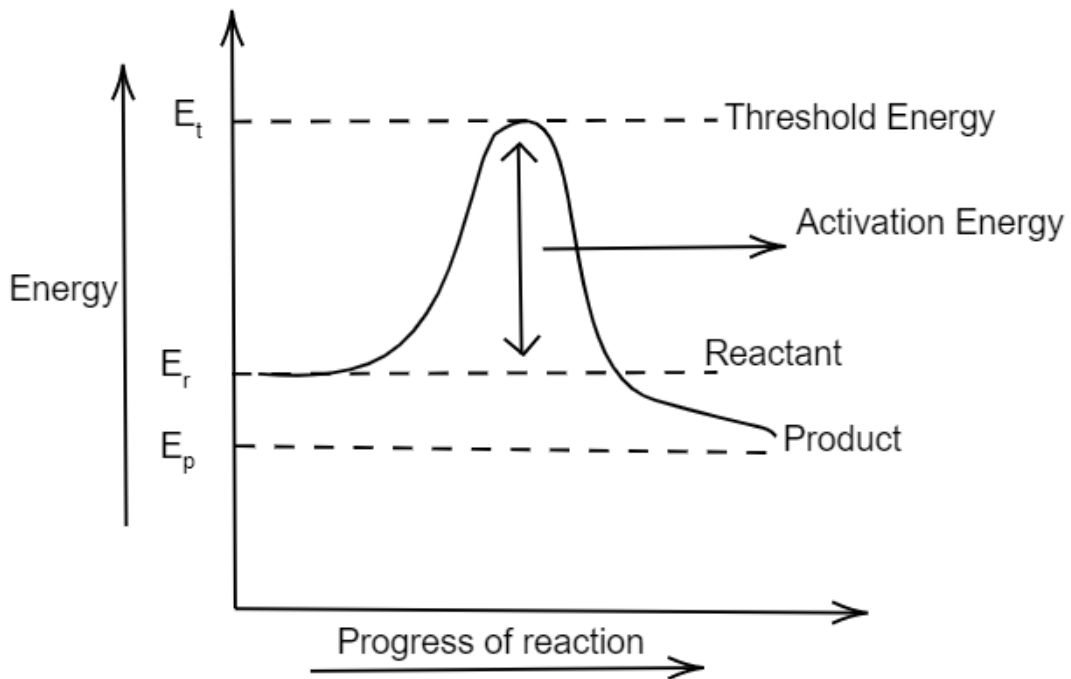
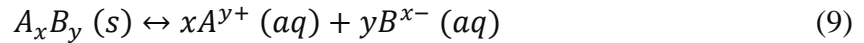


Figure 3.5 Exothermic energy diagram for a reaction [38].

The threshold energy is the minimum amount of energy required to start a particular reaction and is an important step in understanding the kinetics of a reaction. The activation energy acts as a barrier that reactants need to overcome to form products, affecting the rate of scale formation. Thermodynamics, on the other hand, is determined by Gibbs free energy (ΔG), and determines whether a reaction is possible based on energy transformation between reactants and products [10]. As seen in Figure 3.5, the reaction releases energy and becomes spontaneous and exothermic if the product's Gibbs free energy is lower than the reactant's, giving a negative ΔG . Conversely, an endothermic reaction, requiring continuous energy input, occurs when the product's energy is higher than the reactants.

The solubility product constant (K_{sp}) plays an important role in predicting and managing scale formation. Knowledge about the influence that different variables have on the K_{sp} for scale-forming reactions helps predict the likelihood of precipitation or dissolution under specific conditions [39]. K_{sp} quantifies the equilibrium concentration of ions in a saturated solution of a sparingly soluble salt.

Considering the general dissolution reaction in aqueous solutions below:



The K_{sp} is expressed as follows:

$$K_{sp} = [A^{y+}]^x * [B^{x-}]^y \quad (10)$$

K_{sp} helps to determine if the concentration of ions in a solution exceeds the solubility limit which will lead to precipitation of the salt and scale formation. By comparing the product of the concentrations of ions present in a solution at a given moment to the K_{sp} value, we can assess whether conditions favor scale formation or dissolution [40]. If the ion product exceeds K_{sp} , precipitation occurs, causing scale formation. If the ion product is less than K_{sp} , the solution is unsaturated, and the existing scale may dissolve [41]. This understanding improves the prediction and management of scale-related problems in industrial processes.

3.4. Scale Inhibitors

Scale deposition is a problem in the production of oil and gas and requires efficient control techniques. Some of the primary methods are chemical or physical removal techniques, sulfate reduction in injected seawater, and the use of SIs for preventative measures [1]. Preventing scale formation is generally more cost-effective than removing it, and chemical inhibition is the preferred method for maintaining well productivity in most cases. SIs are chemicals added in small amounts to water to delay or prevent scale formation. They are preferred because of their effectiveness at low dosages (several ppm), which offers long-lasting protection for both surface and downhole scale control treatments [26].

SIs work by interfering with the formation or growth of scale deposits [42]. They do this by either preventing scale-forming ions from precipitating out of solution or by stabilizing these ions in a soluble form, preventing them from adhering to surfaces and forming deposits. But for a SI to be able to bind to a scale particle, it either needs to interact with the anions or the cations in the water. Therefore, molecules with several similar functional groups and proper spacing of these groups are needed. One effective way to achieve this is by adding quaternary ammonium, phosphonium, or sulfonium groups to anionic SI polymers, where some of the most common anionic groups are [1]:

- Phosphate ions ($-\text{OPO}_3\text{H}^-$)
- Phosphonate ions ($-\text{PO}_3\text{H}^-$)
- Phosphinate ions ($-\text{PO}_2\text{H}^-$)
- Carboxylate ions ($-\text{COO}^-$)
- Sulfonate ions ($-\text{SO}_3^-$)

These groups are linked to an organic backbone and have good interactions with divalent metals. This can be beneficial to enhance adsorption onto formation rocks.

MIC is the minimum amount of SI that is necessary to inhibit the scale formation at a certain level. An effective SI should have the ability to inhibit or prevent crystal growth at threshold levels. MIC is commonly between 1 and 20 ppm [43].

3.4.1. Mechanism

The exact mechanism of SIs is not fully understood, but they are thought to function in two primary ways: as dispersing/modification agents or stabilizing agents. Crystal dispersing or modification agents (thermodynamic inhibition) chelate or bind to reactants in a soluble form, inhibiting precipitation up to a saturation threshold, thereby preventing crystal adhesion. Because they consume the scale ions in stoichiometric ratios, the efficiency and cost-effectiveness of these types of SI are poor [15]. Stabilization agents (kinetic inhibition), on the other hand, adsorb onto active growth sites of scale crystals on a surface, preventing further growth [44], [45]. In a way, they mimic the ongoing scale formation and inhibit the chance of new scale to form. They are much more effective than dispersing inhibitors as they can inhibit scale formation at concentrations on the order of 1000 times less than a balanced stoichiometric ratio [15]. Both mechanism pathways are illustrated in Figure 3.6.

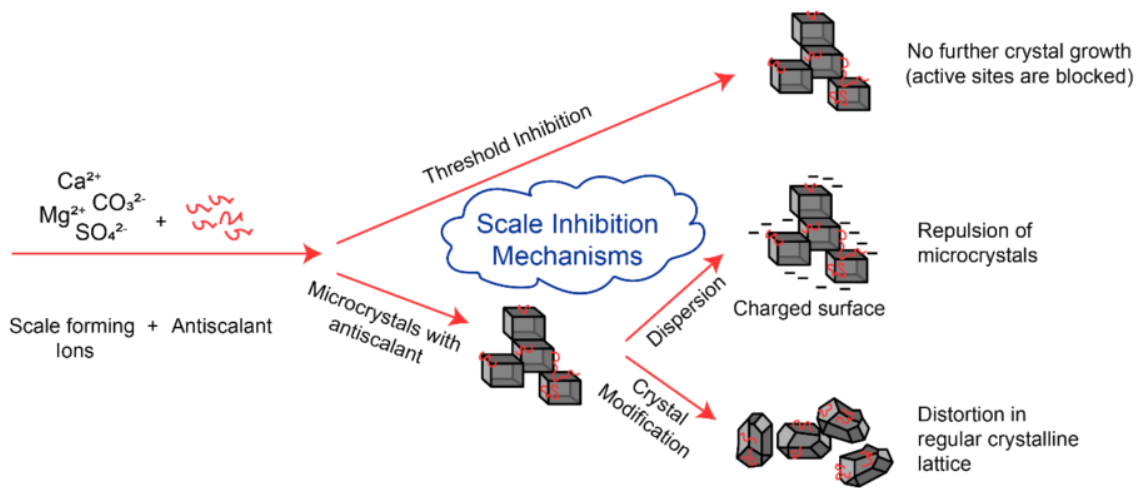


Figure 3.6 Scale inhibition mechanisms [46].

For either subcritical nuclei inhibition or crystal growth inhibition to occur, the SI must bind to a scale particle by interacting with either the anions or cations in the brine. Typically, multiple interactions are required to firmly attach the inhibitor to the surface, necessitating molecules with several similar functional groups and appropriate spacing to interact effectively with the lattice ions on the crystal surface [1]. Since these chemicals work by slowing down the growth of scale crystals, the inhibitor needs to be introduced before precipitation begins. This suggests two basic principles when using SIs: the inhibitor should

be injected upstream of the problematic region, and the inhibitor needs to be consistently present in the water prone to scaling to prevent the growth of each scale crystal as it forms [26].

3.4.2. Phosphonates and Aminophosphonates as Scale Inhibitors

Phosphonates are water-soluble molecules or polymers containing one or more phosphonate-groups. They show a very strong inhibitory effect for preventing mineral scale formation in the oil and gas production system and they are among the most commonly used SIs in scale control [18], [44]. They are extensively used for scales such as calcium carbonates and phosphates, calcium/barium/strontium sulfates and others [47]. Phosphonates function by reducing scale deposition through a combination of crystal dispersion and scale stabilization [15], which hinders their growth and agglomeration [48]. In addition to inhibiting scale formation, phosphonate-based inhibitors can be detected and quantified in produced water, making them easier to monitor. Moreover, their robust adsorption to formation rocks enhances squeeze lifetimes, minimizing well management downtime and enables the utilization of non-polymeric phosphonate molecules [49], [50].

Aminomethylenephosphonic acids are phosphonate-based SIs containing one or more aminomethylenephosphonate groups ($-\text{NH}_2\text{-CH}_2\text{-PO}(\text{OH})_2$). By adding an amine group into a phosphonate molecule enhances the molecule's metal binding capacity through interactions between the amine and phosphonate [1]. The amine group acts as a Lewis base ligand because it can donate a pair of electrons to form a covalent bond with a metal ion. This enhances the inhibitor's ability to bind to the metal surface and inhibit scale formation and forms greater metal ligand complex stability than a phosphonic acid group alone [49]. It has been shown that differences in the carbon chain between nitrogen atoms in amino phosphonic acids affect the interaction of the phosphonic acids with calcite scale where a longer backbone gives a higher effectiveness [51]. Figure 3.7 shows some aminophosphonate SIs commonly used in oilfield scale control.

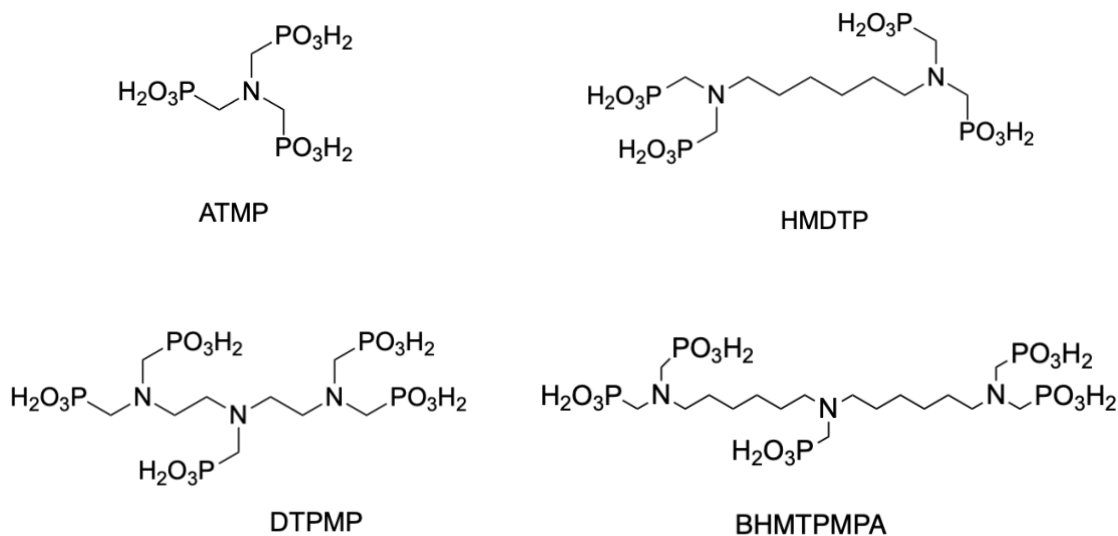


Figure 3.7 Common oilfield aminophosphonate SIs containing aminomethylene-phosphonate groups.

Commercially available aminophosphonate SIs are primarily used for carbonate and sulfate scale inhibition. They are useful in applications for continuous injection but particularly for SI squeeze treatments [49], since they have shown high thermostability [48].

Growing environmental concerns and regulatory restrictions have led to a shift towards the development of green SIs that have high biodegradability, low environmental mobility, and are cost-effective. An ideal profile for environmentally friendly inhibitor systems has been proposed according to the principles of responsible care. This includes [52]:

1. Excellent scale inhibition
2. Low aquatic and human toxicity
3. High biodegradability
4. Low water hazard class (maximum of 2)
5. Good price/performance ratio
6. Free of phosphorous, nitrogen and heavy metals

The discharge of produced water containing nitrogen or phosphorus can lead to an enrichment of nutrients in the environment, resulting in environmental disequilibrium, leading to eutrophication. So, the discharge of phosphonates into the environment can

contribute to unwanted eutrophication in lakes and coastal areas. Most aminophosphonates have low biodegradability, but they are generally low in toxicity and bioaccumulation. However, because of strict environmental regulations, there has been a gradual shift towards replacing aminophosphonates with greener alternatives [1].

To reduce the environmental impact of offshore chemicals, the Oslo and Paris Commission (OSPAR) has developed a harmonized mandatory control procedure for oilfield chemical usage in the North Sea. It has been developed biodegradable polymers in oilfields, but they do not have sufficient thermal stability for downhole squeezing applications [50]. Phosphonate-based inhibitors have on the other hand shown a relatively long squeeze lifetime. This means that they will be effective for a long period after injection into the well [34]. The longer squeeze lifetime can lead to cost savings and operational efficiency by reducing the need for frequent inhibitor reapplications, maintenance downtime, and related costs.

The performance of phosphonate SIs is well known, and these SIs have been proven to effectively control scale deposition in oil wells. This ensures smooth production operation, and in addition, these SIs are cost-effective [53].

Phosphonate SIs have been important resources in the oil industry because of these factors. The decision to phase them out should be considered due to their benefits, which include improved scale prevention, cost savings, and operational efficiency. Balancing environmental concerns with operational needs is important for sustainable and efficient oil production. Therefore, it could be an option to use phosphonate-based SIs until a greener alternative with comparable qualities is available on the market.

3.4.2.1. Calcium Compatibility

There are many performance tests and key factors that must be considered when selecting a SI, but one important factor is its compatibility with calcium. Phosphonate-based SIs often face challenges due to their limited compatibility with calcium ions [50]. Generally, phosphonates have a high tolerance for calcium ions, but since they usually are applied in systems with high calcium ion concentrations in the water, the phosphonates react stoichiometrically with the calcium ions. This forms insoluble calcium–phosphonate

complexes or precipitates which share some of the same harmful effects as the scale aimed to be inhibited [54]. Metal-inhibitor precipitates like this pose a serious problem in process streams and can compromise SIs performance and accelerate overall scale formation [55], [56].

3.4.2.2. Oxidation of Aminophosphonates

It has been shown that amine oxides with hydroxyl groups can give advantages such as better water-solubility and highly favorable compatibility with other surfactants [57], [58]. Thus, oxidizing aminophosphonates into oxides can potentially improve their calcium compatibility in scale inhibition. This modification introduces hydrophilic groups, making the molecules more soluble in water and less likely to precipitate with calcium ions.

Another potential advantage of oxidizing aminophosphonates is the increased stability it offers in the presence of hypochlorite ions from biocides. Aminophosphonates are sensitive to oxidative degradation in the presence of chlorine compounds commonly used in biocides or disinfectants. These are used when controlling microbiological growth in industrial water systems that also use scale inhibitors for scale control [47]. Using aminophosphonate oxides with at least one oxidized tertiary amine group has shown to be less sensitive to calcium and more stable in the presence of chlorine [59].

Because of this, they have been suggested to be used against corrosion as well. Phosphates, polyphosphates, and phosphonates are attractive to use in corrosion control as they are relatively non-toxic, but they also face challenges with calcium compatibility [60]. Aminophosphonate oxides provide strong corrosion inhibition for iron-based metals, making them a valuable alternative to traditional highly toxic inorganic corrosion inhibitors [61]. Thus, oxidized aminophosphonates can be used in various water systems against both scale and corrosion, even in waters with high calcium content and those treated with chlorine-based biocides.

3.5. Application of Scale Inhibitors

In the oilfield industry, SIs are used through various methods to prevent the formation of scale deposits. These methods include [62]:

- Batch treatment
- Continuous injection
- Squeeze treatment

Table 3.1 [29] gives an overview of the advantages and disadvantages of each technique.

Table 3.1 Advantages and disadvantages of SI application techniques [29].

Method	Advantages	Disadvantages
Batch treatment	<ul style="list-style-type: none"> • Chemical costs and labor requirements are reduced • More effective for non-carbonate reservoirs • More effective for strongly leaching inhibitors, in particularly polyester-based inhibitors • Minimized shutdown production • Less time-consuming 	<ul style="list-style-type: none"> • Production stops during treatments • Short lifetimes
Continuous injection	<ul style="list-style-type: none"> • Chemical costs and labor requirements are reduced • More effective for non-carbonate reservoirs • More effective for strongly leaching inhibitors, in particularly polyester-based inhibitors • Minimized shutdown production • Less time-consuming • Can be done in combination with other treatments, for example, a mixture of scale and corrosion inhibitors, foaming agents, cleaning agents, etc. 	<ul style="list-style-type: none"> • Relative more expensive • Ineffective where there is a considerable inhibitor retention on the rock matrix • Sensitive to inter-well distances, i.e., considered to be effective only where inter-well distances are relatively short
Squeeze treatment (adsorption and precipitation squeezes)	<ul style="list-style-type: none"> • More effective in carbonate reservoirs • Cost-effective method for slowly leaching inhibitors, in particularly phosphonate inhibitors • Ensures a long lifetime, inhibition may be prolonged to 24 months after treatment • Minimizes periodical treatments 	<ul style="list-style-type: none"> • Ineffective for non-carbonate reservoirs • Not the best option for strongly leaching inhibitors • Production stops during treatments • May cause formation damage • Time-consuming, several steps are involved

3.5.1. Batch Treatment

This method involves using a significant amount of SI over time, added regularly. The top of the pipe is pumped with large volumes of SIs, which are then pushed to the bottom of the pipe by the oil well fluids. The well needs to be shut down for a certain amount of time during this treatment before the production can start again [29]. This is problematic as the technique requires regular implementation on a weekly or monthly basis. It also has to be taken into account that a corrosion inhibitor must be present when aqueous fluids like SIs are in contact with wellbore completion [62].

3.5.2. Continuous Injection

In this method, the SI is injected with a capillary tubular. The SI is injected at the surface and transported downhole by a surface pump [11]. It then flows through the production tubular to prevent it from scale formation [62]. To achieve a homogeneous mixture after the addition of the SI, it is introduced at the point of turbulence, with a constant supply maintained at a controlled rate. The specific concentration required for inhibition of scale is monitored closely to ensure that the SI performance is highly efficient [29].

The added SI will adhere to the rock matrix until the rock's absorptive capacity is reached. As a result, the inhibitor concentration in the solution will not increase before the absorptive capacity is reached. This period, known as the retardation time of the rock matrix, makes the inhibition ineffective. Factors such as the type of rock matrix, brine chemistry, and concentration of injected inhibitor will affect the retardation time [29], [63]. Given this, continuous injection is preferred when the SI used has low adsorption to the formation [64]. Figure 3.8 shows a standard chemical injection system for an offshore platform.

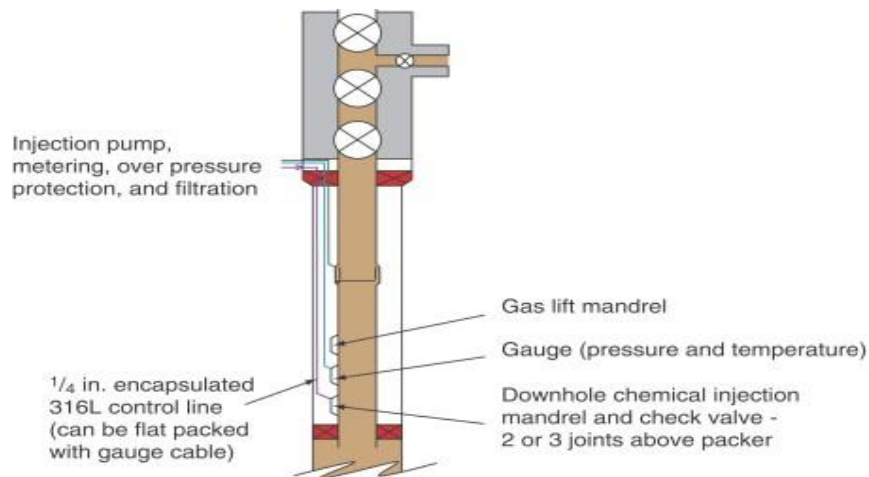


Figure 3.8 Illustration of downhole continuous injection [65].

3.5.3. Squeeze Treatment

For many years, squeeze treatment with SIs has been the preferred method for preventing or managing scale formation and its following deposition [5]. As illustrated in Figure 3.9, the process involves pumping fluids containing the SI into the formation and then shutting in the well for some hours to enable the inhibitor to adsorb onto the formation rock. This method is designed to place a significant amount of chemicals within the reservoir, ensuring a gradual release into the produced water over several months. Normally the concentration of SIs that are forced through the wellbore ranges between 2.5 % and 20 % by weight. This gradual release gives sufficient concentration to prevent scaling when the production is restarted [1].

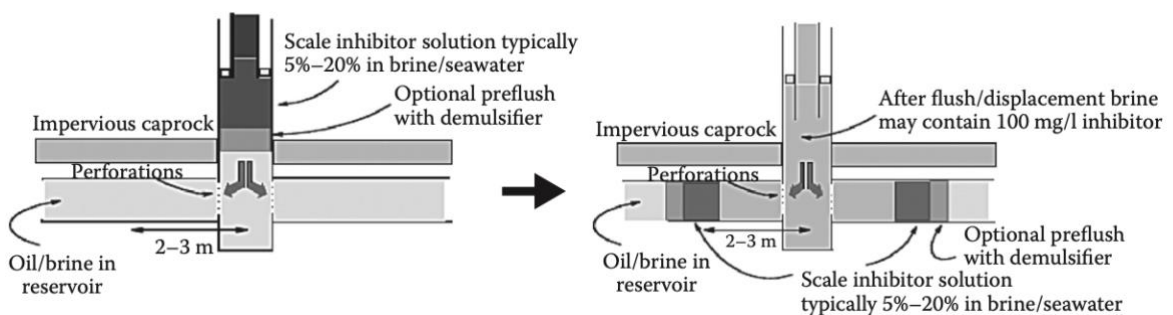


Figure 3.9 Squeeze treatment of SIs [1].

The water's concentration of SI will gradually decrease, and the well is re-squeezed when it reaches a level where complete scale control is not achieved [66].

Squeeze treatment designs follow five stages [67], [68]:

1. Preflush squeeze: A preliminary step for formation rock condition.
2. Main treatment: Injection of concentrated SI into the formation.
3. Overflush: Designed to push and position the SI into a desired depth into the formation, approximately 3-5 ft away from the wellbore.
4. Shut-in period: Period where the SI is allowed to adsorb onto the formation rock.
5. Production resumption: The well is put back into production, and the SI return profile is monitored.

Figure 3.10 illustrates the three main steps of a scale squeeze treatment in a uniformly pressured well with homogeneous permeability [69].

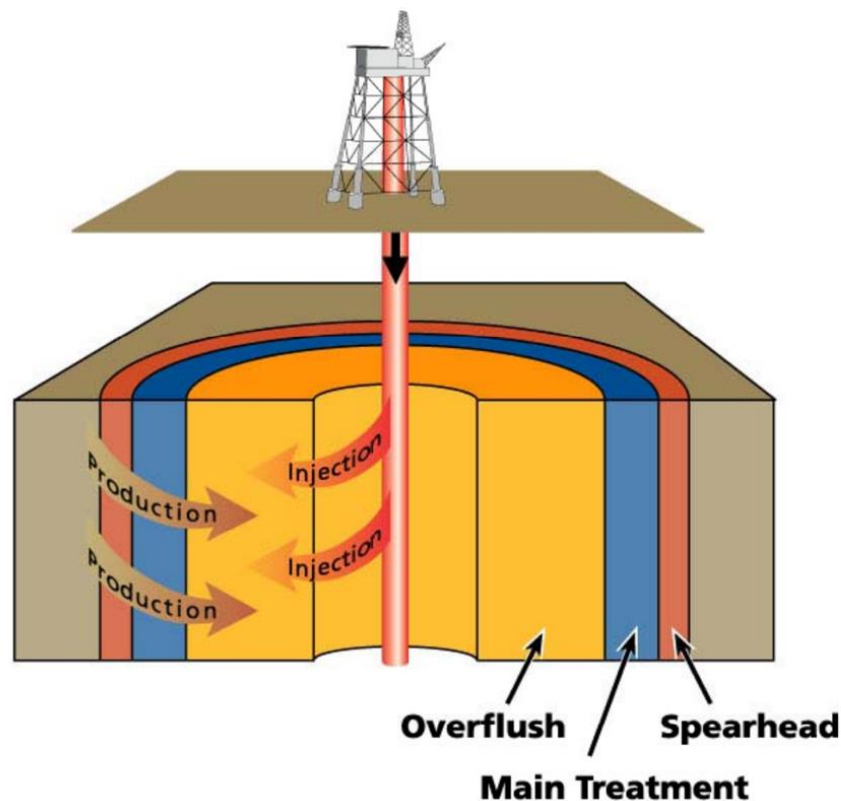


Figure 3.10 Schematic illustration of the main steps of a scale squeeze treatment [69].

The most critical factor in squeeze treatment design is the squeeze lifetime. This is determined by the days of production or volume of water where the chemical return concentration is higher than the MIC [43]. To optimize down-hole squeezing, the SI needs to adsorb onto the formation rock, preventing early washout of the chemical [5]. It should have an adsorption isotherm that rises quickly at first, then flattens out as the concentration increases [70] meaning that a lot of the SI can stick to the formation and still be in equilibrium with a solution that has a low inhibitor concentration. SIs containing phosphonate groups are highly advantageous for squeeze treatments due to their strong adsorption onto rock formations, which results in long squeeze lifetimes and reduces the downtime required for well management [50], [66].

However, long-term scale inhibition relies not only on the adsorption of the inhibitor onto formation rock but also on its subsequent desorption for it to migrate into the well. Therefore, it is important to consider the desorption rate of the SI for squeeze treatment, instead of only focusing on how well it adsorbs [71]. A SI with a flat and low adsorption isotherm that desorbs quickly is usually preferable over one with a steep slope. This is because even though the SI may initially adhere strongly, it may not provide long-lasting protection if it doesn't release efficiently or is irreversibly adsorbed. A SI with a faster desorption rate could offer more sustained protection against scale formation in the long run despite weaker adsorption properties. Thus, finding a balance between strong adsorption and rapid desorption is important to ensure long-lasting protection and optimal scale inhibition performance as the life of a squeeze job is mostly based on the kinetics of the adsorption-desorption process [72]. Figure 3.11 show a typical desorption isotherm model. By measuring the SI return data from performed squeeze treatments, concentration can be plotted over time to give a desorption plot.

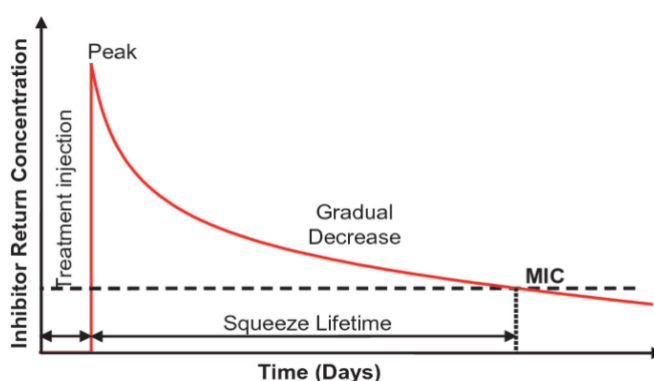


Figure 3.11 Desorption isotherm model [73].

Several methods have been established to improve the squeeze lifetime by increasing the retention of SIs on rock formation. Some of them are [1]:

- Precipitation squeeze treatment
- Use of some transition metal ions and Zn^{2+} ions
- Raising the pH *in situ*
- Mutual solvents to change the rock wettability
- Blends with cationic polymers
- Incorporating cationic monomers in the SI polymer structure
- Cross-linked SIs
- Use of kaolinite or other clay that enhances inhibitor adsorption
- SI microparticles

In addition to desorption, another challenge associated with squeeze treatments is to make sure that the SIs used can tolerate high-pressure and temperature conditions. As well depths increase, the injected chemicals are exposed to these conditions for longer periods. Temperatures ranging from 180-200 °C and pressures over 10,000 psi are common in deep wells. Therefore, it is crucial to evaluate the impact of increased temperature and pressure on the performance of SIs using chemical analytical techniques and product performance methods [74], [75]. The SIs used in squeeze treatment must not degrade under such conditions.

4. Experimental

4.1. Chemicals and Equipment

All the chemicals used for this study are purchased from Italmatch Chemicals, Aquapharm, VWR and Sigma-Aldrich.

For nuclear magnetic resonance (NMR) spectroscopy an Ascend™ 400 from BRUKER was used. Analytical balance is an Adventurer™ from OHAUS and the drying and heating oven is from BINDER. The Scale Rig 5000 from Scaled Solutions was used for high-pressure dynamic tube blocking testing.

4.2. Synthesis

In the synthesis of SIs, four different types of aminophosphonates were oxidized by adding hydrogen peroxide (H_2O_2). The performance of these modified SIs was compared with the non-oxidized aminophosphonates as reference.

The synthesis of aminophosphonate oxides involved the addition of a 30 wt% H_2O_2 solution as the oxidizing agent. The precise quantity of H_2O_2 added to each aminophosphonate was determined through stoichiometric and gravimetric calculations. The accurate amounts of chemicals were then added to a container using an analytical balance. The solutions were mixed for at least 24 hours at room temperature, using a magnetic stirrer. Some solutions were oxidized in a 60 °C heat bath to evaluate whether increased temperature was necessary for achieving complete oxidation. Figure 4.1-4.4 illustrates the oxidation reactions for the aminophosphonates used.

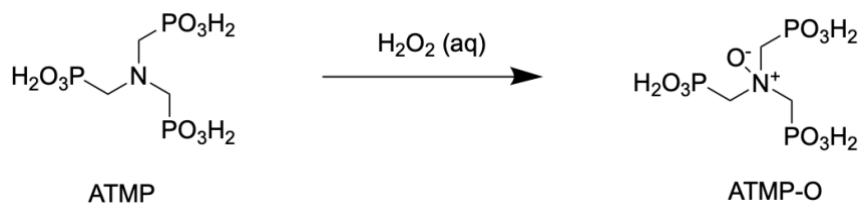


Figure 4.1 Oxidation of amino-tris (methylenephosphonic acid), sodium salt.

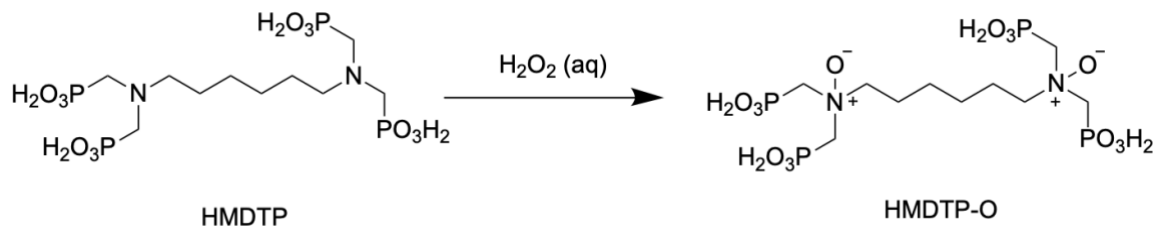


Figure 4.2 Oxidation of hexamethylenediamine tetra(methylenephosphonic acid), potassium salt.

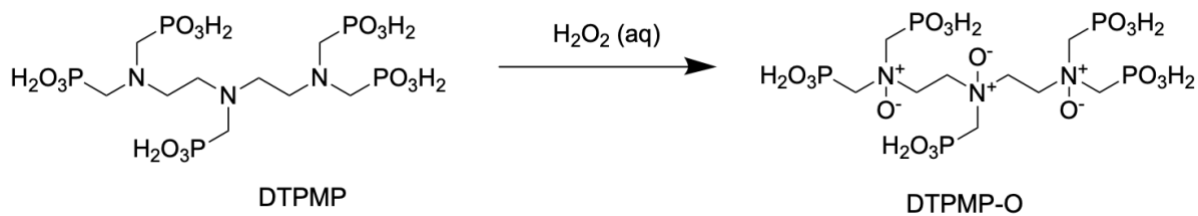


Figure 4.3 Oxidation of diethylenetriamine penta(methylphosphonic) acid, sodium salt.

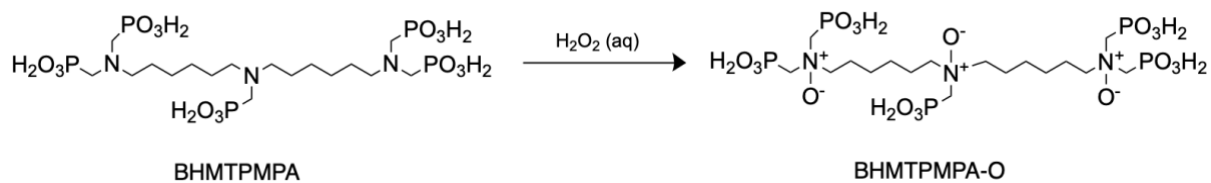


Figure 4.4 Oxidation of bis(hexamethylene triamine)penta(methylenephosphonic acid).

4.2.1. pH Adjustment

The pH levels of the aminophosphonates varied from 2 to 11. Both the oxidized and non-oxidized aminophosphonates were tested as SIs at their original pH. For those with low initial pH values, an additional test was performed after pH adjustment to pH 6. This adjustment aimed to improve the comparability of the results among the various aminophosphonates. The pH was adjusted by adding a NaOH solution until the desired pH level was reached. It was tried to adjust the pH both before and after oxidation to see its impact on the oxidation process.

4.3. Characterization of SIs

Nuclear magnetic resonance (NMR) spectroscopy was used for chemical characterization and reaction validation. The spectra were obtained using a 400 MHz Bruker NMR spectrometer, with ^{31}P chemical shifts analyzed in deuterium oxide (D_2O).

4.4. High-Pressure Dynamic Tube Blocking Test Protocol

Scaled Solutions offers testing capabilities of SIs with the high-pressure dynamic tube blocking scale rig Scale Rig 5000 (Figure 4.5). The rig is made for testing temperatures up to 200 °C and pressure up to 300 bars. Dynamic scale testing allows for high-quality testing of SI performance at high temperature and pressure conditions which will simulate the real conditions present during oil production. All the data is collected on a computer and the rig is controlled by using Scaled Solutions Ltd – USB Data Logger.



Figure 4.5 Picture of the dynamic tube-blocking scale rig.

The setup consists of three pumps, each responsible for pumping certain aqueous solutions at a specified flow rate at maximum 10 mL/min in total. Pumps 1 and 2 deliver aqueous solutions of cations and anions, respectively, while pump 3 is responsible for the inhibitor solution. Pump 2 is also used for the cleaning solutions which are ethylenediaminetetraacetic acid (EDTA) solution and distilled water. All solutions mix before they enter a coil positioned within an oven for controlled heating. The coil is made of 316 stainless steel and measures 3 meters in length with an internal diameter of 1 millimeter. This system enables measurement of pressure differentials across the scaling coil. Figure 4.6 shows a schematic diagram of the scale rig.

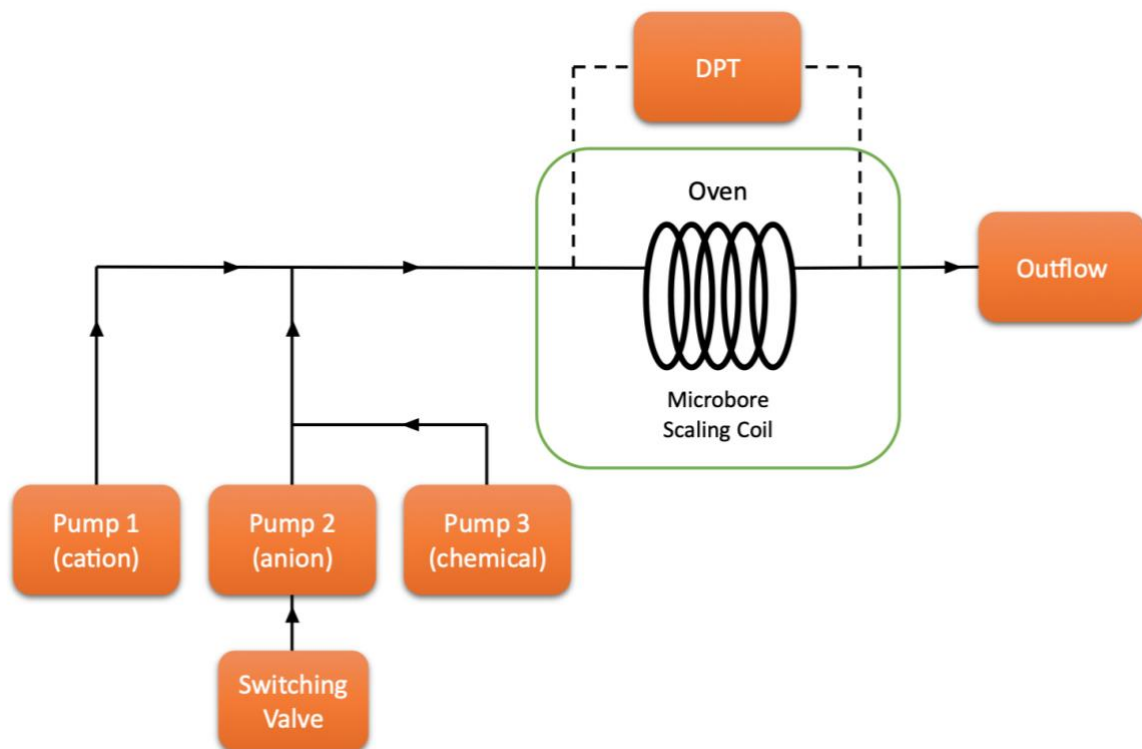


Figure 4.6 Schematic diagram of the high-pressure dynamic tube-blocking scale rig.

The synthetic brines used in this experiment are based on seawater and water produced in the Heidrun oilfield in Norway. Minerals and salts are dissolved in distilled water to the compositions given in Table 4.1 below. To avoid air bubbles entering the tubing in the scale rig, all the brines were degassed after they were made.

Table 4.1 Salt composition of brine 1 and brine 2 for calcite and barite scale.

Ion	Component	Calcite			Barite		
		Brine 1 (g/3 L)	Brine 2 (g/3 L)	Conc. (ppm)	Brine 1 (g/3 L)	Brine 2 (g/3 L)	Conc. (ppm)
Na ⁺	NaCl	148.77	148.77	39202	115.92	105.12	19510
Ca ²⁺	CaCl ₂ .2H ₂ O	22.45		2040	15.93		2040
Mg ²⁺	MgCl ₂ .6H ₂ O	13.30		530	40.98		530
K ⁺	KCl	6.23		1090	5.76		1090
Ba ²⁺	BaCl ₂ .2H ₂ O	3.04		570	1.53		570
Sr ²⁺	SrCl ₂ .6H ₂ O	2.65		290	1.32		290
HCO ₃ ⁻	NaHCO ₃		8.26	1000			
SO ₄ ²⁻	Na ₂ SO ₄					13.14	2960

For testing of the SIs, the Scale Rig 5000 was set to 100 °C and 80 bars. All inhibitor solutions were made to solutions with a concentration of 1000 ppm. The automated scale rig is set to conduct three consecutive tests during each test run:

- Blank: Contains only cation and anion brines and continues until scale forms and stops when the differential pressure exceeds 10 psi.
- Chemical: Runs 1-hour long tests with different inhibitor concentrations starting at the highest concentration and decreasing. It continues until the tube is blocked within 1 hour (differential pressure exceeds 10 psi) which is the failed inhibitor concentration (FIC). The concentrations are 100, 50, 20, 10, 5, 2 and 1 ppm.
- Repeat chemical: Repeats the last successful inhibitor concentration test which is the MIC followed by a test at the FIC.

After a tube block, the scale is removed from the system before it can continue to the next test. This is done by washing for 10 minutes with EDTA-solution followed by 10 minutes of distilled water.

The results are collected from the differential pressure data and can be illustrated graphically as shown in Figure 4.7 below.

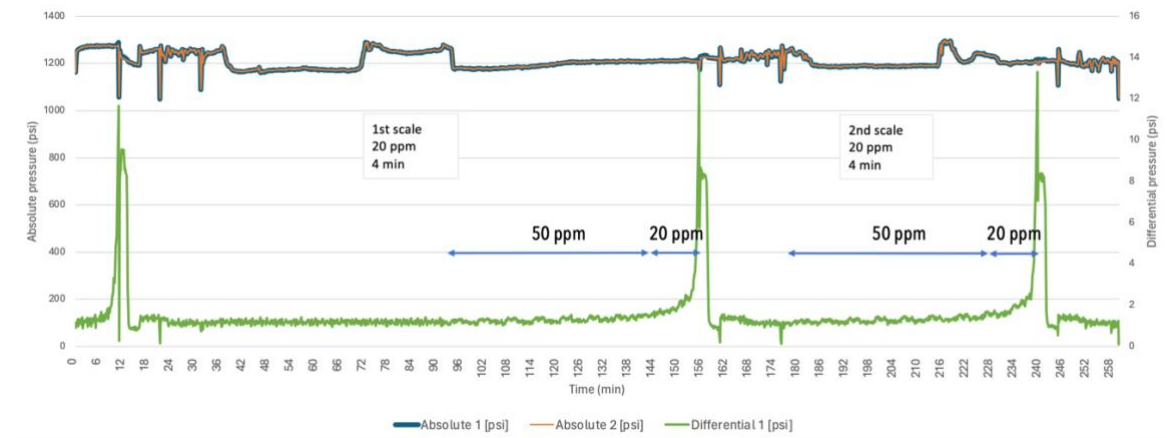


Figure 4.7 Graphical illustration of the results of a SI test.

4.4.1. Problems with High-Pressure Dynamic Tube Blocking Scale Rig

Some problems were occurring while using the scale rig. The first issue was air bubbles in the system. These bubbles caused a pressure drop by blocking the flow of the solution through the scale rig. These bubbles were first removed by using a syringe, but often new bubbles continued to form. The filters were old, but there was no new filter available to change to. Therefore, this issue was solved by removing the filters before each test, washing them with distilled water, and drying them with paper. This usually fixed the problem, but a few times it was needed to put the filters in an ultrasonic cleaner for a few seconds to prevent the formation of air bubbles.

Another problem occurred when the system washed after tube blockage caused by calcite scale. The original washing program was set to 7 ml/min in 5 minutes and then 9.99 ml/min in 5 minutes of EDTA solution, which resulted in the differential pressure exceeding 30 psi, causing the system to automatically abort the test. Each time this happened, it was needed to manually wash the machine and restart the test. To fix this problem, the washing program with EDTA solution was changed to 5 ml/min in 4 minutes, 7 ml/min in 3 minutes, then 9.99 ml/min in 5 minutes. This adjustment prevented the pressure from reaching as high differential pressure, allowing the washing process to continue without automatically aborting.

4.5. Calcium Compatibility Test

The compositions of ions in water vary a lot for the different oilfields. In oilfields with high levels of calcium ions, the compatibility of SIs with calcium is crucial. The prevalence of high calcium levels in oilfields often results in the precipitation of calcium complexes, reducing production efficiency. Using SIs with low affinity for calcium ions is essential in these oilfields to minimize this challenge.

Calcium compatibility testing was performed on the commercial and synthesized SIs to evaluate if the oxidation resulted in reduced incompatibility. The tests were performed following a procedure from Energy & Fuels [66]. Different inhibitor concentrations were added to solutions with varying concentrations of calcium to examine the occurrence of precipitation.

Four different concentrations of SIs (100ppm, 1000ppm, 10000ppm and 50000ppm) were added to assigned bottles. Following that, calcium solution was added to respective bottles with concentrations of 100ppm, 1000ppm and 10000ppm. This gave a total of 12 bottles. The bottles were shaken and placed in the oven at 70 °C. The bottles were checked for precipitation after mixing, 30 minutes, 1 hour, 4 hours and 24 hours. Figure 4.8 shows an example of various bottles from the compatibility test.

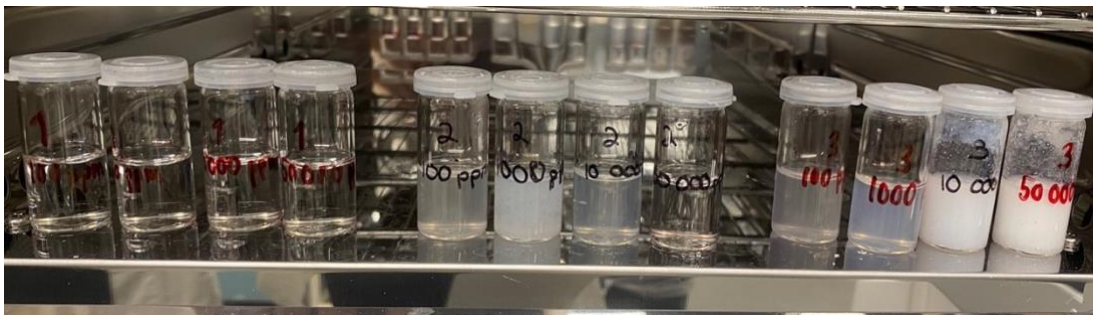


Figure 4.8 Example of calcium compatibility test.

4.6. Thermal Stability Test

A thermal aging test was conducted to evaluate the stability and performance of the SIs under high-temperature conditions, simulating conditions for squeeze treatment. A 5-10 wt% solution of SI in deionized water at pH 6 was prepared in a pressure tube, and then nitrogen gas was used to remove the excess oxygen. The tubes were then placed in a heated oil bath with continuous stirring for one week (Figure 4.9). The test was performed twice for each SIs at 140 °C and 160 °C, respectively. The inhibition performance of the aged inhibitors was tested using the scale rig and compared with the non-aged inhibitors. Both the commercial and synthesized SIs underwent this procedure.



Figure 4.9 Picture of an ongoing thermal aging test.

5. Results and Discussion

The experimental results are presented and discussed in the following section. The primary objective of these experiments was to determine if oxidizing aminophosphonates improves their compatibility with calcium ions. The oxidized SIs were compared to their equivalent non-oxidized commercial SIs. Four different commercial SIs were selected for testing and oxidation. The chemical compositions of the SIs were identified by using ^{31}P NMR spectroscopy to characterize the compounds and verify their oxidation. For detailed NMR spectra, see Appendix A-1.

5.1. High-Pressure Dynamic Tube Blocking Test

All SIs were tested on the high-pressure dynamic tube blocking scale rig at 80 bars and 100 °C against both calcite and barite scales. The detailed procedure is described in chapter 4.3. FIC was tested twice for consistency reasons and is listed as “first scale” and “second scale” together with the time indicating how long the test ran before it was blocked with scale.

For improved comparability, tube blocking test results for SIs at pH 6 are presented together, followed by results at other pH levels.

5.1.1. pH 6

The results for the SIs at pH 6 against calcite scale are presented in Table 5.1. First scale and second scale FICs correlate nicely for all tests indicating that the results are reliable. BHMTMPMA has two different FICs, 1 and 2 ppm, but given that the test ran for 50 minutes into 2 ppm and only 8 minutes into 1 ppm, the time difference makes it acceptable.

Table 5.1 FIC values all SIs at pH 6 against calcite scale.

SI	First Scale		Second Scale	
	Time (min)	Conc. (ppm)	Time (min)	Conc. (ppm)
ATMP	11	1	11	1
ATMP-O	17	2	35	2
ATMP-O*	6	2	22	2
HMDTP	-	<1	-	<1
HMDTP-O	-	<1	-	<1
DTPMP	26	2	26	2
DTPMP-O	13	2	25	2
DTPMP-O**	10	2	21	2
BHMTMPMA	50	2	8	1
BHMTMPMA-O	21	2	30	2
BHMTMPMA-O**	19	2	23	2

* Oxidated in an oil bath at 60 °C.

** pH adjusted before oxidation.

Figure 5.1 shows the FIC results for ATMP-O against calcite scale graphically through plotting the differential pressure of the scaling coil over time. The FIC is recognized as the two last peaks which represent when the tube is blocked with scale.

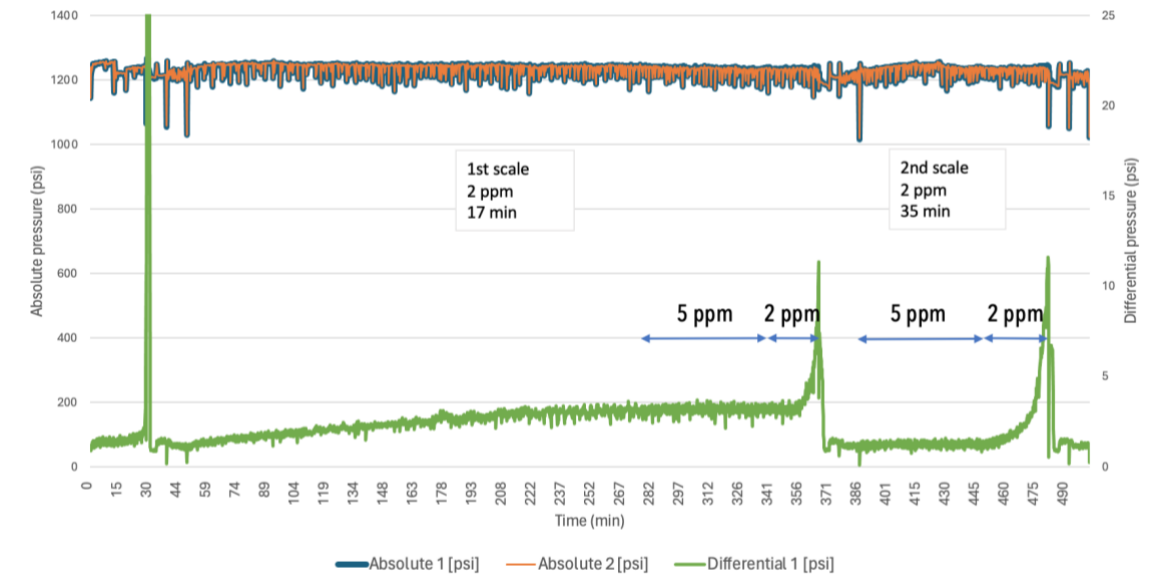


Figure 5.1 FIC results of ATMP-O against calcite scale.

Out of the SIs at pH 6 against calcite scale, HMDTP show the highest inhibition performance in both the commercial and oxidized form by passing the lowest concentration of 1 ppm. All other SIs has a slight decrease in inhibitory efficiency after oxidation, where ATMP has decreased the most. However, ATMP had the second-best inhibitory effect (after HMDTP) with a FIC of 1 ppm. All other SIs has an FIC of about 2 ppm.

The results for the SIs at pH 6 against barite scale are presented in Table 5.2. First scale and second scale FICs correlate perfectly for all tests indicating that the results are reliable.

Table 5.2 FIC values all SIs at pH 6 against barite scale.

SI	First Scale		Second Scale	
	Time (min)	Conc. (ppm)	Time (min)	Conc. (ppm)
ATMP	29	20	30	20
ATMP-O	4	20	4	20
ATMP-O*	45	50	42	50
HMDTP	17	10	21	10
HMDTP-O	33	20	34	20
DTPMP	25	10	26	10
DTPMP-O	8	10	11	10
DTPMP-O**	17	20	18	20
BHMTPMPA	9	5	10	5
BHMTPMPA-O	52	10	47	10
BHMTPMPA-O**	4	10	2	10

* Oxidated in an oil bath at 60 °C.

** pH adjusted before oxidation.

Figure 5.2 shows the FIC results for ATMP-O against barite scale graphically through plotting the differential pressure of the scaling coil over time. Again, the FIC is recognized as the two last peaks which represent when the tube is blocked with scale.

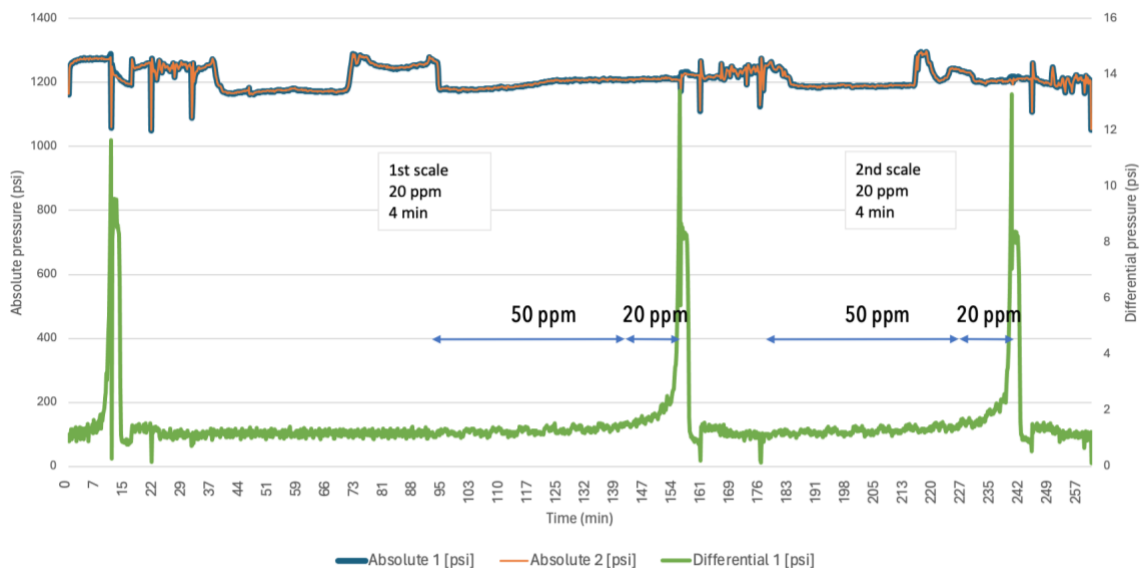


Figure 5.2 FIC results of ATMP-O against barite scale.

BHMTMPMPA showed the best inhibition performance on the barite scale with a FIC of 5 ppm after 9 and 10 minutes after the first and second scales, respectively. BHMTMPMPA-O has the best effect out of the oxidized ones with a FIC of 10 ppm after 52 and 47 minutes after the first and second scale, respectively. The SIs number of phosphonate groups affects the inhibition performance. An earlier study performed by Bromley et al. reported SIs had a highly improved barite prevention with an increasing number of phosphonate groups [76], [77]. The results were therefore expected, with ATMP having the worst inhibition effect, and BHMTMPMPA the best.

On calcite scale, HMDTP showed both the best inhibition performance out of all SIs but also the least decrease in effect after oxidation. On barite scale on the other hand, HMDTP does not only not have the best inhibitory effect in its commercial form but also the highest decrease in effect after oxidation. This shows that even if a SI works well for one type of scale, it may not necessarily work well for another type.

Generally, pH has been adjusted after the oxidation reaction of the SIs. We therefore wanted to investigate the impact of adjusting the pH before oxidation, which was done for DTPMP and BHMTMPMPA. For calcite scale, no significant difference is seen, suggesting no difference in the oxidation reaction after pH adjustment. For barite scale on the other hand, both SIs show a slight decrease in inhibition performance. Because both DTPMP and

BHMTMPMPA showed reduced inhibition performance after oxidation compared to their commercial forms, we would expect a general reduction of inhibition efficiency after oxidation. In that case, this performance decrease could suggest that pH adjustment before oxidation leads to a more complete oxidation reaction. A possible explanation for that is the presence of protons (H^+) in the solution. When the pH is low, the concentration of protons in the solution is high. This could lead to protonation of the aminophosphonates, possibly making them less susceptible to oxidation. Hence, adjusting the pH before oxidation could improve conditions for efficient oxidation with hydrogen peroxide.

Oxidation in an oil bath at 60 °C was also done to investigate the impact the temperature has on the oxidation process and was executed for ATMP. The results on both calcite and barite scales show a small decrease in its performance compared to oxidation at room temperature. As ATMP shows a reduced inhibition performance after oxidation compared to its commercial form, we would expect a general reduction of inhibition efficiency after oxidation in this case as well. This decrease in performance could again suggest that oxidation in an oil bath at 60 °C leads to a more complete oxidation reaction.

5.1.2. Various pH Levels

First and second scale FIC values correlate well for all tests (calcite and barite) indicating that the results are reliable. The results for the SIs at varying pH levels against calcite scale are presented in Table 5.3.

Table 5.3 FIC values all SIs at varying pH against calcite scale.

SI	pH (1000 ppm)	First Scale		Second Scale	
		Time (min)	Conc. (ppm)	Time (min)	Conc. (ppm)
ATMP	2-3	12	1	7	1
ATMP-O	2	44	2	52	2
ATMP	7-8	-	<1	-	<1
ATMP-O	7-8	-	<1	-	<1
ATMP-O(AQUACID)	8	8	2	22	2
DTPMP	3	15	2	25	2
DTPMP-O	3	26	2	27	2
BHMTMPMPA	2	9	1	24	1
BHMTMPMPA-O	2	31	2	36	2

In general, all SIs show good inhibitory effect against calcite scale. ATMP and ATMP-O (oxidized in the lab) at pH 7-8 both had no scale formation at 1 ppm and is even more effective than at pH 6. At pH 2-3, DTPMP, BHMTMPMPA and their oxidized forms show the same or slightly better performance than for pH 6 against calcite scale.

The results for the SIs at varying pH levels against barite scale are presented in Table 5.4.

Table 5.4 FIC values all SIs at varying pH against barite scale.

SI	pH (1000 ppm)	First Scale		Second Scale	
		Time (min)	Conc. (ppm)	Time (min)	Conc. (ppm)
ATMP	2-3	14	100	14	100
ATMP-O	2	13	100	13	100
ATMP	7-8	10	10	18	10
ATMP-O	7-8	7	10	11	10
ATMP-O(AQUACID)	8	11	20	13	20
DTPMP	3	49	100	47	100
DTPMP-O	3	15	50	17	50
BHMTMPMPA	2	11	100	11	100
BHMTMPMPA-O	2	10	100	10	100

ATMP, ATMP-O and ATMP-O (AQUACID) at pH 7-8 show good inhibitory efficiency against barite scale with FIC values at 10, 10 and 20 ppm respectively. They are more effective than ATMP and ATMP-O at pH 6. However, at pH 2-3, both the oxidized and commercial forms did not work at all, with a FIC of 100 ppm. DTPMP, BHMTMPMPA and BHMTMPMPA-O also showed no effectiveness at pH 2-3 each with FIC values of 100 ppm. Interestingly enough, DTPMP-O at pH 3 is more effective than its commercial form with a FIC at 50 ppm, but still less effective than at pH 6.

These results show just how big of a role the pH levels play on the performance of SIs. Carbonate scales are pH-sensitive, and CaCO_3 gets more soluble in acidic conditions. This will give fewer free calcium ions available to form scale, which can explain why the SIs have good performance at lower pH. Barite on the other hand is pH-independent, and the reason for the reduced SI performance at lower pH can be explained by protonation of the SI. This reduces their ability to bind effectively with barium ions, which then will reduce their efficacy to prevent the formation of barite scale.

Another research [78] has also tested ATMP and DTPMP on the scale rig using the same type of brines, pressure and temperature, but with a pH range between 5 and 7. This study reported that the FIC for ATMP was 20 ppm for calcite and 10 ppm for barite. For DTPMP,

the FIC values were 10 ppm for calcite and 5 ppm for barite. These results differ from the results given in the tables above. One possible explanation for the variation in FIC for the barite scale can be explained by the small difference in pH. It has been seen in this study and others that a lower pH significantly affects the performance of the SIs against barite negatively [79] and that a higher pH gives a lower FIC [80]. The pH value is not accurate as it is only measured using pH strips. If the pH of ATMP and DTPMP was on the higher end of the stated range in Mady et al. study, this could be the reason for better inhibition performance compared to the results in this study at pH 6. In addition, both studies have confirmed that DTPMP with higher molecular weight will give better inhibition compared to the smaller molecule ATMP.

For calcite, the difference in FIC values is more challenging to explain. Both ATMP and DTPMP had better performance for all pH values in this study compared to Mady et al. Possible factors that can contribute to such differences can be variations in inhibitor preparation or the purity of the inhibitors used. Scale accumulation in the coil could also play a role. In this study, the coil was changed to a new one, giving no build-up to affect the results. If the used coil is old with pre-existing scale build-up, it could possibly give a higher initial differential pressure, reaching the FIC faster.

5.2. Calcium Compatibility Test

One of the most important factors of squeeze treatment is the compatibility of SIs with calcium ions [50]. Many SIs tend to interact with the brine in the reservoirs to form complexes with calcium ions. The precipitation of the SIs as a result of this interaction can cause problems with oil production operations. In order to evaluate the calcium compatibility of various SIs, a series of tests were conducted, following the procedure in Chapter 4.4. Both the commercial and oxidized SIs were tested. The results were evaluated using a rating scale with the categories “terrible”, “very bad”, “bad”, “medium”, “good”, “very good”, “excellent” and “perfect”. Detailed results for all SIs can be found in Appendix A-3. Table 5.5 presents a summary of the results from the calcium compatibility tests for all SIs at pH 6.

The results indicate a trend where SIs with longer carbon backbones are more compatible with calcium ions. This trend is consistent for both commercial and oxidized SIs, indicating that calcium compatibility is influenced by molecular structure. The smallest molecules ATMP and ATMP-O showed bad compatibility with calcium. ATMP-O oxidized in oil bath also showed bad compatibility, suggesting that a more complete oxidation will not affect the SIs calcium compatibility. In contrast, HMDTP, HMDTP-O, DTPMP, and DTPMP-O with higher molecular weight showed good calcium compatibility. The biggest molecules BHMTMPMPA and BHMTMPMPA-O had very good compatibility with calcium, making them the preferable choices in terms of calcium tolerance.

A small improvement was noted for HMDTP when it was oxidized (HMDTP-O), but the overall compatibility between oxidized and commercial SIs showed negligible differences.

Table 5.5 Summary of calcium compatibility for all SIs at pH 6.

SI	Calcium Compatibility
ATMP	Bad
ATMP-O	Bad
ATMP-O*	Bad
HMDTP	Good
HMDTP-O	Good – very good
DTPMP	Good
DTPMP-O	Good
BHMTMPMPA	Very good
BHMTMPMPA-O	Very good

* Oxidated in an oil bath at 60 °C.

Calcium compatibility tests were also performed on SIs with different pH, summarized in Table 5.6. The SIs with low pH, both commercial and oxidized, showed perfect or excellent calcium compatibility. This can be explained due to calcium ions remaining in their free ionic form at lower pH levels, which do not precipitate with the SI. At low pH, the phosphonate groups on the SIs are more likely to be protonated. This will also reduce their ability to bind to calcium ions, which results in lower chances of forming insoluble precipitates. This will be the opposite for higher pH, giving very poor calcium compatibility.

Table 5.6 Summary of calcium compatibility for all SIs at varying pH.

SI	pH	Calcium Compatibility
ATMP	2-3	Excellent
ATMP-O	2	Perfect
ATMP	7-8	Terrible
ATMP-O	7-8	Very bad
ATMP-O (AQUACID)	8	Bad
DTPMP	3	Perfect
DTPMP-O	3	Perfect
BHMTMPMPA	2	Perfect
BHMTMPMPA-O	2	Perfect

5.3. Thermal Stability Test

A thermal stability test was conducted to evaluate the potential of using SIs in squeeze treatments, which require long-term thermal stability. The tests were performed according to the method described in 4.5. The results of the thermal aging test at 140 °C are presented in Tables 5.7 and 5.8, and at 160 °C in Tables 5.9 and 5.10.

Table 5.7 FIC values all SIs at pH 6 against calcite scale after thermal aging at 140 °C.

SI	First Scale		Second Scale	
	Time (min)	Conc. (ppm)	Time (min)	Conc. (ppm)
ATMP	56	2	6	1
ATMP-O	6	2	19	2
HMDTP	-	<1	-	<1
HMDTP-O	13	2	27	2
DTPMP	23	2	34	2
DTPMP-O	10	2	22	2
BHMTMPMPA	30	1	34	1
BHMTMPMPA-O	11	2	25	2

Table 5.8 FIC values all SIs at pH 6 against barite scale after thermal aging at 140 °C.

SI	First Scale		Second Scale	
	Time (min)	Conc. (ppm)	Time (min)	Conc. (ppm)
ATMP	49	20	55	20
ATMP-O	41	50	42	50
HMDTP	5	5	9	5
HMDTP-O	1	20	3	20
DTPMP	18	10	19	10
DTPMP-O	26	50	25	50
BHMTMPMPA	18	10	23	10
BHMTMPMPA-O	51	20	1	10

Table 5.9 FIC values all SIs at pH 6 against calcite scale after thermal aging at 160 °C.

SI	First Scale		Second Scale	
	Time (min)	Conc. (ppm)	Time (min)	Conc. (ppm)
ATMP	19	1	24	1
ATMP-O	14	2	30	2
HMDTP	<1	-	<1	-
HMDTP-O	8	2	28	2
DTPMP	8	1	8	1
DTPMP-O	14	2	25	2
BHMTPMPA	19	1	10	1
BHMTPMPA-O	14	2	23	2

Table 5.10 FIC values all SIs at pH 6 against barite scale after thermal aging at 160 °C.

SI	First Scale		Second Scale	
	Time (min)	Conc. (ppm)	Time (min)	Conc. (ppm)
ATMP	39	20	39	20
ATMP-O	32	50	35	50
HMDTP	53	10	59	10
HMDTP-O	2	20	1	20
DTPMP	20	20	20	20
DTPMP-O	10	50	16	50
BHMTPMPA	14	10	19	10
BHMTPMPA-O	3	10	42	20

The results showed that after thermal aging, the SIs mostly maintained their inhibition efficiency compared to the results presented in Tables 5.1 and 5.2. For ATMP, there was no difference observed after thermal aging, while ATMP-O showed consistent performance for calcite but lost inhibition efficiency for barite, increasing the FIC from 20 ppm to 50 ppm. After thermal aging, HMDTP showed a small improvement for barite, and maintained the same efficiency for calcite. For HMDTP-O the FIC increased after

thermal aging for calcite from <1 ppm to 2 ppm, while the FIC for barite was constant. After thermal aging at 160 °C, DTPMP showed a lower FIC for calcite, decreasing from 2 ppm to 1 ppm, but its performance for barite got worse, with the FIC increasing from 10 ppm to 20 ppm. DTPMP-O maintained its performance for calcite but became less effective for barite, as the FIC increased from 10 ppm to 50 ppm at both 140 °C and 160 °C. BHMTMPMPA retained the same inhibitory efficiency for calcite, but the FIC for barite increased from 5 ppm to 10 ppm at 140 °C and 160 °C. BHMTMPMPA-o showed no change in inhibition performance after thermal aging for both calcite and barite.

These results indicate that even though most SIs maintain their function as inhibitors at high temperatures, some variations were seen, especially for the oxidized forms. For example, thermal aging reduced the performance of ATMP-O and DTPMP-O. This can indicate that they might not be as thermally stable as the non-oxidized forms. On the other hand, HMDTP and its oxidated form showed good stability and even slightly improved performance, and BHMTMPMPA and BHMTMPMPA-O also showed great thermal stability.

6. Conclusion

The aim of this study was to oxidize the commercial aminophosphonate SIs ATMP, HMDTP, DTPMP and BHMTMPMPA into aminophosphonate oxides to improve their calcium compatibility. Both the commercial and oxidized forms were tested for calcium compatibility, thermal stability, and inhibition performance using a high-pressure tube blocking rig.

Overall, all inhibitors demonstrated effective inhibition properties against calcite scale at pH 6, though there was a slight decrease in effectiveness after oxidation. The exception was HMDTP and its oxide, which exhibited excellent inhibitory effects even at the lowest concentration of 1 ppm. For barite scale at pH 6, the oxidized inhibitors also show a general slight decrease in inhibitory effect compared to their commercial forms. A notable trend was that larger inhibitor molecules exhibited better inhibition properties against barite scale.

In calcium compatibility testing, results indicated that SIs with longer carbon backbones were more compatible with calcium ions than those with shorter carbon backbones. The largest molecules, BHMTMPMPA and its oxide, had the best calcium compatibility, while the smallest molecules, ATMP and its oxide, had the worst. Additionally, HMDTP was the only inhibitor that demonstrated a slight compatibility improvement after oxidation. In conclusion, most SIs showed little or no improvement after oxidation.

Thermal aging results indicated that most SIs maintained their function as inhibitors at high temperatures. Although the oxides generally performed worse compared to their commercial forms, their performance remained acceptable. Considering both calcite and barite scales, HMDTP, BHMTMPMPA and their oxides exhibited the best stability.

Even though HMDTP-O showed better calcium compatibility compared to HMDTP, both BHMTMPMPA and BHMTMPMPA-O had equally good calcium compatibility. However, due to the poorer inhibition performance of BHMTMPMPA-O compared to the commercial, it is not the best alternative. When comparing HMDTP-O and BHMTMPMPA, HMDTP-O has a slightly better inhibition performance for calcite before thermal aging, but worse against barite. After thermal aging, HMDTP-O has a FIC of 2 ppm for calcite and 20 ppm for barite, whereas BHMTMPMPA has a FIC of 1 ppm for calcite and 10 ppm for barite. Therefore, BHMTMPMPA is the preferred SI if barite is an issue at the site. However, HMDTP-O can

also be a good option if calcite is the main problem. The environmental impact should then be considered; if HMDTP-O is effective at lower or similar concentrations compared to BHMTMPMA, it could lead to reduced chemical usage. Additionally, HMDTP-O has a lower phosphorus and nitrogen content, which can reduce the environmental impact.

In conclusion, when choosing HMDTP-O and BHMTMPMA both the scale type and environmental impact should be considered. As HMDTP-O is effective at lower concentrations and has lower phosphorus and nitrogen content, it could reduce chemical usage and environmental impact, making it a sustainable alternative.

References

- [1] M. A. Kelland, *Production chemicals for the oil and gas industry*, Second Edition. CRC Press Inc, 2014.
- [2] G. Li, S. Guo, J. Zhang, og Y. Liu, «Inhibition of scale buildup during produced-water reuse: Optimization of inhibitors and application in the field», *Desalination*, bd. 351, s. 213–219, okt. 2014, doi: 10.1016/j.desal.2014.08.003.
- [3] E. J. Mackay, «Modeling In-Situ Scale Deposition: The Impact of Reservoir and Well Geometries and Kinetic Reaction Rates», *SPE Production & Facilities*, bd. 18, nr. 01, s. 45–56, feb. 2003, doi: 10.2118/81830-PA.
- [4] I. R. Collins, «A New Model for Mineral Scale Adhesion», presentert på International Symposium on Oilfield Scale, OnePetro, jan. 2002. doi: 10.2118/74655-MS.
- [5] A. A. Olajire, «A review of oilfield scale management technology for oil and gas production», *Journal of Petroleum Science and Engineering*, bd. 135, s. 723–737, nov. 2015, doi: 10.1016/j.petrol.2015.09.011.
- [6] A. Spinthaki *mfl.*, «Searching for a universal scale inhibitor: A multi-scale approach towards inhibitor efficiency», *Geothermics*, bd. 89, s. 101954, jan. 2021, doi: 10.1016/j.geothermics.2020.101954.
- [7] M. S. Kamal, I. Hussein, M. Mahmoud, A. S. Sultan, og M. A. S. Saad, «Oilfield scale formation and chemical removal: A review», *Journal of Petroleum Science and Engineering*, bd. 171, s. 127–139, des. 2018, doi: 10.1016/j.petrol.2018.07.037.
- [8] M. F. Mady, «Chapter 16 - Oilfield scale inhibitors: Synthetic and performance aspects», i *Water-Formed Deposits*, Z. Amjad og K. D. Demadis, Red., Elsevier, 2022, s. 325–352. doi: 10.1016/B978-0-12-822896-8.00033-9.
- [9] J. Fink, «Chapter 7 - Scale inhibitors», i *Petroleum Engineer's Guide to Oil Field Chemicals and Fluids (Third Edition)*, J. Fink, Red., Gulf Professional Publishing, 2021, s. 351–391. doi: 10.1016/B978-0-323-85438-2.00007-4.
- [10] S. Kumar, T. K. Naiya, og T. Kumar, «Developments in oilfield scale handling towards green technology-A review», *Journal of Petroleum Science and Engineering*, bd. 169, s. 428–444, okt. 2018, doi: 10.1016/j.petrol.2018.05.068.
- [11] G. M. Graham, E. J. Mackay, S. J. Dyer, og H. M. Bourne, «The Challenges for Scale Control in Deepwater Production Systems: Chemical Inhibition and Placement», 2002.
- [12] W. W. Frenier og M. Ziauddin, «A Multifaceted Approach for Controlling Complex Deposits in Oil and Gas Production», presentert på SPE Annual Technical Conference and Exhibition, OnePetro, sep. 2010. doi: 10.2118/132707-MS.

- [13] J. Li, M. Tang, Z. Ye, L. Chen, og Y. Zhou, «Scale formation and control in oil and gas fields: A review», *Journal of Dispersion Science and Technology*, bd. 38, nr. 5, s. 661–670, mai 2017, doi: 10.1080/01932691.2016.1185953.
- [14] A. Hussein, «Chapter 5 - Mineral Scales in Oil and Gas Fields», i *Essentials of Flow Assurance Solids in Oil and Gas Operations*, A. Hussein, Red., Gulf Professional Publishing, 2023, s. 199–296. doi: 10.1016/B978-0-323-99118-6.00004-6.
- [15] M. C. Aberdeen *mfl.*, «Fighting Scale — Removal and Prevention», 2000. Åpnet: 27. februar 2024. [Online]. Tilgjengelig på: <https://www.semanticscholar.org/paper/Fighting-Scale-%E2%80%94-Removal-and-Prevention-Aberdeen-Scotland/5dddcdc5e89e335bacdf40bd1de0f7768c480ba8>
- [16] C. D. Team, «Water Formed Scale - Common Scaling Types in Refineries», FQE Chemicals. Åpnet: 27. februar 2024. [Online]. Tilgjengelig på: <https://fqechemicals.com/water-formed-scale/>
- [17] O. J. Vetter og W. A. Farone, «Calcium Carbonate Scale in Oilfield Operations», presentert på SPE Annual Technical Conference and Exhibition, OnePetro, sep. 1987. doi: 10.2118/16908-MS.
- [18] H. Wang, Y. Zhou, Q. Yao, S. Ma, W. Wu, og W. Sun, «Synthesis of fluorescent-tagged scale inhibitor and evaluation of its calcium carbonate precipitation performance», *Desalination*, bd. 340, s. 1–10, mai 2014, doi: 10.1016/j.desal.2014.02.015.
- [19] Q. Wang *mfl.*, «Laboratory study on efficiency of three calcium carbonate scale inhibitors in the presence of EOR chemicals», *Petroleum*, bd. 4, nr. 4, s. 375–384, des. 2018, doi: 10.1016/j.petlm.2018.03.003.
- [20] K. Ramstad, T. Tydal, K. M. Askvik, og P. Fotland, «Predicting Carbonate Scale in Oil Producers From High-Temperature Reservoirs», *SPE Journal*, bd. 10, nr. 04, s. 363–373, des. 2005, doi: 10.2118/87430-PA.
- [21] A. Taha og M. Amani, «Water Chemistry in Oil and Gas Operations: Scales Properties and Composition», *International Journal of Organic Chemistry*, bd. 9, nr. 3, Art. nr. 3, jul. 2019, doi: 10.4236/ijoc.2019.93012.
- [22] J. Al-Ashhab, H. Al-Matar, og S. Mokhtar, «Techniques Used to Monitor and Remove Strontium Sulfate Scale in UZ Producing Wells», presentert på Abu Dhabi International Petroleum Exhibition and Conference, OnePetro, nov. 2006. doi: 10.2118/101401-MS.
- [23] A. B. B. Merdhah og Abu Azam Mohd Yassin, «Barium Sulfate Scale Formation in Oil Reservoir During Water Injection at High-Barium Formation Water», *Journal of Applied Sciences*, bd. 7, nr. 17, s. 2393–2403, doi: 10.3923/jas.2007.2393.2403.
- [24] M. Amiri og J. Moghadasi, «The Effect of Temperature, Pressure, and Mixing Ratio of Injection Water with Formation Water on Barium Sulfate Scale Formation in Siri Oilfield»,

Energy Sources, Part A: Recovery, Utilization, and Environmental Effects, bd. 35, nr. 14, s. 1316–1327, jul. 2013, doi: 10.1080/15567036.2010.516322.

[25] Y. Liu, Z. Dai, A. T. Kan, M. B. Tomson, og P. Zhang, «Investigation of sorptive interaction between phosphonate inhibitor and barium sulfate for oilfield scale control», *Journal of Petroleum Science and Engineering*, bd. 208, s. 109425, jan. 2022, doi: 10.1016/j.petrol.2021.109425.

[26] Y. Bai og Q. Bai, «17 - Subsea Corrosion and Scale», i *Subsea Engineering Handbook (Second Edition)*, Y. Bai og Q. Bai, Red., Boston: Gulf Professional Publishing, 2019, s. 455–487. doi: 10.1016/B978-0-12-812622-6.00017-8.

[27] O. J. G. Vetter, «How Barium Sulfate Is Formed: An Interpretation», *Journal of Petroleum Technology*, bd. 27, nr. 12, s. 1515–1524, des. 1975, doi: 10.2118/4217-PA.

[28] Y. M. Al-Roomi og K. F. Hussain, «Potential kinetic model for scaling and scale inhibition mechanism», *Desalination*, bd. 393, s. 186–195, sep. 2016, doi: 10.1016/j.desal.2015.07.025.

[29] M. Mpelwa og S.-F. Tang, «State of the art of synthetic threshold scale inhibitors for mineral scaling in the petroleum industry: a review», *Pet. Sci.*, bd. 16, nr. 4, s. 830–849, aug. 2019, doi: 10.1007/s12182-019-0299-5.

[30] M. Safari, A. Golsefatan, og M. Jamialahmadi, «Inhibition of Scale Formation Using Silica Nanoparticle», *Journal of Dispersion Science and Technology*, bd. 35, okt. 2014, doi: 10.1080/01932691.2013.840242.

[31] S. Lee og C. H. Lee, «Scale formation in NF/RO: mechanism and control», *Water Science and Technology*, bd. 51, nr. 6–7, s. 267–275, mar. 2005.

[32] S. Lee og C.-H. Lee, «Effect of operating conditions on CaSO₄ scale formation mechanism in nanofiltration for water softening», *Water Research*, bd. 34, nr. 15, s. 3854–3866, okt. 2000, doi: 10.1016/S0043-1354(00)00142-1.

[33] A. Antony, J. H. Low, S. Gray, A. E. Childress, P. Le-Clech, og G. Leslie, «Scale formation and control in high pressure membrane water treatment systems: A review», *Journal of Membrane Science*, bd. 383, nr. 1, s. 1–16, nov. 2011, doi: 10.1016/j.memsci.2011.08.054.

[34] S. Baraka-Lokmane, K. Sorbie, N. Poisson, og N. Kohler, «Can Green Scale Inhibitors Replace Phosphonate Scale Inhibitors?: Carbonate Coreflooding Experiments», *Petroleum Science and Technology*, bd. 27, nr. 4, s. 427–441, mar. 2009, doi: 10.1080/10916460701764605.

[35] A. B. BinMerdhah, A. A. M. Yassin, og M. A. Muherei, «Laboratory and prediction of barium sulfate scaling at high-barium formation water», *Journal of Petroleum Science and Engineering*, bd. 70, nr. 1, s. 79–88, jan. 2010, doi: 10.1016/j.petrol.2009.10.001.

- [36] A. Shokrollahi, H. Safari, Z. Esmaeili-Jaghdan, M. H. Ghazanfari, og A. H. Mohammadi, «Rigorous modeling of permeability impairment due to inorganic scale deposition in porous media», *Journal of Petroleum Science and Engineering*, bd. 130, s. 26–36, jun. 2015, doi: 10.1016/j.petrol.2015.03.013.
- [37] A. T. Kan og M. B. Tomson, «Scale Prediction for Oil and Gas Production», *SPE Journal*, bd. 17, nr. 02, s. 362–378, feb. 2012, doi: 10.2118/132237-PA.
- [38] «Draw graph which is used to calculate the activation energy of a reaction. Write the appropriate equation used to calculate the activation energy graphically.» Åpnet: 8. mai 2024. [Online]. Tilgjengelig på: <https://www.vedantu.com/question-answer/draw-graph-which-is-used-to-calculate-the-class-11-chemistry-cbse-6148b10ad2f0267fd64dd81d>
- [39] B. Coto, C. Martos, J. L. Peña, R. Rodríguez, og G. Pastor, «Effects in the solubility of CaCO₃: Experimental study and model description», *Fluid Phase Equilibria*, bd. 324, s. 1–7, jun. 2012, doi: 10.1016/j.fluid.2012.03.020.
- [40] R. J. Ferguson, B. R. Ferguson, og R. F. Stancavage, «Modeling Scale Formation and Optimizing Scale Inhibitor Dosages in Membrane Systems».
- [41] «18.1: Solubility Product Constant, K_{sp}», Chemistry LibreTexts. Åpnet: 31. mai 2024. [Online]. Tilgjengelig på: [https://chem.libretexts.org/Bookshelves/General_Chemistry/Map%3A_General_Chemistry_\(Petrucci_et_al.\)/18%3A_Solubility_and_Complex-Ion_Equilibria/18.1%3A_Solubility_Product_Constant_Ksp](https://chem.libretexts.org/Bookshelves/General_Chemistry/Map%3A_General_Chemistry_(Petrucci_et_al.)/18%3A_Solubility_and_Complex-Ion_Equilibria/18.1%3A_Solubility_Product_Constant_Ksp)
- [42] A. T. Kan, Z. Dai, og M. B. Tomson, «The state of the art in scale inhibitor squeeze treatment», *Pet. Sci.*, bd. 17, nr. 6, s. 1579–1601, des. 2020, doi: 10.1007/s12182-020-00497-z.
- [43] O. Vazquez, I. Fursov, og E. Mackay, «Automatic optimization of oilfield scale inhibitor squeeze treatment designs», *Journal of Petroleum Science and Engineering*, bd. 147, s. 302–307, nov. 2016, doi: 10.1016/j.petrol.2016.06.025.
- [44] M. B. Tomson, G. Fu, M. A. Watson, og A. T. Kan, «Mechanisms of Mineral Scale Inhibition», *SPE Production & Facilities*, bd. 18, nr. 03, s. 192–199, aug. 2003, doi: 10.2118/84958-PA.
- [45] K. D. Demadis, «Combating Heat Exchanger Fouling and Corrosion Phenomena in Process Waters», *Proceeding of Compact Heat Exchangers and Enhancement Technology for the Process Industries - 2003*, Åpnet: 23. februar 2024. [Online]. Tilgjengelig på: https://www.academia.edu/3692699/Combating_Heat_Exchanger_Fouling_and_Corrosion_Phenomena_in_Process_Waters
- [46] «Scale Inhibitors», REDA Water. Åpnet: 10. mai 2024. [Online]. Tilgjengelig på: <https://redawater.com/scale-inhibitors/>

- [47] K. D. Demadis og A. Ketsetzi, «Degradation of Phosphonate-Based Scale Inhibitor Additives in the Presence of Oxidizing Biocides: “Collateral Damages” in Industrial Water Systems», *Separation Science and Technology*, mai 2007, doi: 10.1080/01496390701290532.
- [48] Y. A. Issabayev *mfl.*, «Synthesis of unexplored aminophosphonic acid and evaluation as scale inhibitor for industrial water applications», *Journal of Water Process Engineering*, bd. 22, s. 192–202, apr. 2018, doi: 10.1016/j.jwpe.2017.12.007.
- [49] M. F. Mady og M. A. Kelland, «Overview of the Synthesis of Salts of Organophosphonic Acids and Their Application to the Management of Oilfield Scale», *Energy Fuels*, bd. 31, nr. 5, s. 4603–4615, mai 2017, doi: 10.1021/acs.energyfuels.7b00708.
- [50] M. F. Mady, P. Bayat, og M. A. Kelland, «Environmentally Friendly Phosphonated Polyetheramine Scale Inhibitors—Excellent Calcium Compatibility for Oilfield Applications», *Ind. Eng. Chem. Res.*, bd. 59, nr. 21, s. 9808–9818, mai 2020, doi: 10.1021/acs.iecr.0c01636.
- [51] C. Y. Chen, M. Z. Xia, og F. Y. Wang, «Influence of Three Organic Phosphonates on Calcite Crystal Growth», *Advanced Materials Research*, bd. 154–155, s. 437–442, 2011, doi: 10.4028/www.scientific.net/AMR.154-155.437.
- [52] D. Hasson, H. Shemer, og A. Sher, «State of the Art of Friendly “Green” Scale Control Inhibitors: A Review Article», *Ind. Eng. Chem. Res.*, bd. 50, nr. 12, s. 7601–7607, jun. 2011, doi: 10.1021/ie200370v.
- [53] Y. Hu, C. Chen, og S. Liu, «State of art bio-materials as scale inhibitors in recirculating cooling water system: a review article», *Water Science and Technology*, bd. 85, nr. 5, s. 1500–1521, jan. 2022, doi: 10.2166/wst.2022.027.
- [54] B. Zhang, L. Zhang, F. Li, W. Hu, og P. M. Hannam, «Testing the formation of Ca–phosphonate precipitates and evaluating the anionic polymers as Ca–phosphonate precipitates and CaCO₃ scale inhibitor in simulated cooling water», *Corrosion Science*, bd. 52, nr. 12, s. 3883–3890, des. 2010, doi: 10.1016/j.corsci.2010.07.037.
- [55] Z. Amjad, R. T. Landgraf, J. L. Penn, og Walsh University, Division of Mathematics and Sciences, North Canton OH 44720, USA., «Calcium sulfate dihydrate (gypsum) scale inhibition by PAA, PAPEMP, and PAA/PAPEMP blend», *Int. J. Corros. Scale Inhib.*, bd. 3, nr. 1, s. 035–047, 2014, doi: 10.17675/2305-6894-2014-3-1-035-047.
- [56] K. D. Demadis, N. Stavgianoudaki, G. Grossmann, M. Gruner, og J. L. Schwartz, «Calcium–Phosphonate Interactions: Solution Behavior and Ca²⁺ Binding by 2-Hydroxyethylimino-bis(methylenephosphonate) Studied by Multinuclear NMR Spectroscopy», *Inorg. Chem.*, bd. 48, nr. 9, s. 4154–4164, mai 2009, doi: 10.1021/ic802400r.
- [57] R. Wang, Y. Li, og Q. Li, «Synthesis and Properties of Dodecyldiethoxylamine Oxide», *J Surfact Deterg*, bd. 16, nr. 4, s. 509–514, jul. 2013, doi: 10.1007/s11743-013-1460-6.

- [58] H. Liu, G. Shi, B. Xu, S. Chen, og G. Zhang, «Synthesis, Characterization and Properties of N-Alkyl-N,N-di(2-hydroxyethyl) Amine Oxides», *J Surfact Deterg*, bd. 20, nr. 1, s. 129–136, jan. 2017, doi: 10.1007/s11743-016-1900-1.
- [59] C. M. Hwa, J. A. Kelly, J. Neton, P. M. Scanlon, og R. R. Gaudette, «Control of scale in aqueous systems using certain phosphonomethyl amine oxides», EP0432664A1, 19. juni 1991 Åpnet: 29. mai 2024. [Online]. Tilgjengelig på: <https://patents.google.com/patent/EP0432664A1/en?q=EP0432664A1>
- [60] Y. Liu og P. Zhang, «Review of Phosphorus-Based Polymers for Mineral Scale and Corrosion Control in Oilfield», *Polymers*, bd. 14, nr. 13, Art. nr. 13, jan. 2022, doi: 10.3390/polym14132673.
- [61] C. M. Hwa, J. A. Kelly, J. Neton, P. M. Scanlon, og R. R. Gaudette, «Control of corrosion in aqueous systems using certain phosphonomethyl amine oxides», EP0437722A1, 24. juli 1991 Åpnet: 29. mai 2024. [Online]. Tilgjengelig på: <https://patents.google.com/patent/EP0437722A1/en?q=EP0437722A1>
- [62] F. Alissa, R. Altowairqi, K. Alhamed, og A. Alsubaie, «Evaluation of Various Designs for Scale Inhibition Squeeze Treatments in Carbonate Reservoirs», presentert på SPE Annual Technical Conference and Exhibition, OnePetro, sep. 2022. doi: 10.2118/210316-MS.
- [63] E. J. Mackay, «Scale Inhibitor Application in Injection Wells to Protect Against Damage to Production Wells: When Does It Work?», presentert på SPE European Formation Damage Conference, OnePetro, mai 2005. doi: 10.2118/95022-MS.
- [64] J. Bellarby, «Chapter 7 Production Chemistry», i *Developments in Petroleum Science*, bd. 56, i Well Completion Design, vol. 56. , Elsevier, 2009, s. 371–432. doi: 10.1016/S0376-7361(08)00207-0.
- [65] A. D. Shirah, M. C. Place, og M. A. Edwards, «Reliable Sub-Sea Umbilical and Down-Hole Injection Systems are an Integral Component of Successful Flow Assurance Programs», presentert på SPE Annual Technical Conference and Exhibition, OnePetro, okt. 2003. doi: 10.2118/84046-MS.
- [66] M. F. Mady, P. Charoensumran, H. Ajiro, og M. A. Kelland, «Synthesis and Characterization of Modified Aliphatic Polycarbonates as Environmentally Friendly Oilfield Scale Inhibitors», *Energy Fuels*, bd. 32, nr. 6, s. 6746–6755, jun. 2018, doi: 10.1021/acs.energyfuels.8b01168.
- [67] B. Ghosh og X. Li, «Effect of surfactant composition on reservoir wettability and scale inhibitor squeeze lifetime in oil wet carbonate reservoir», *Journal of Petroleum Science and Engineering*, bd. 108, s. 250–258, aug. 2013, doi: 10.1016/j.petrol.2013.04.012.
- [68] O. Vazquez, E. Mackay, K. Sorbie, og M. Jordan, «Impact of Mutual Solvent Preflush on Scale Squeeze Treatments: Extended Squeeze Lifetime and Improved Well Clean-up Time», presentert på 8th European Formation Damage Conference, OnePetro, mai 2009. doi:

10.2118/121857-MS.

[69] M. M. Jordan, E. J. Mackay, og O. Vazquez, «The Influence Of Overflush Fluid Type On Scale Squeeze Life Time - Field Examples And Placement Simulation Evaluation», presentert på CORROSION 2008, OnePetro, mar. 2008. Åpnet: 19. april 2024. [Online]. Tilgjengelig på: <https://dx.doi.org/>

[70] J. K. Kerver og J. K. Heilhecker, «Scale Inhibition by the Squeeze Technique», *Journal of Canadian Petroleum Technology*, bd. 8, nr. 01, s. 15–23, jan. 1969, doi: 10.2118/69-01-03.

[71] J. L. Przybylinski, «Adsorption and Desorption Characteristics of Mineral Scale Inhibitors as Related to the Design of Squeeze Treatments», presentert på SPE International Symposium on Oilfield Chemistry, OnePetro, feb. 1989. doi: 10.2118/18486-MS.

[72] O. J. Vetter, «The Chemical Squeeze Process Some New Information on Some Old Misconceptions», *Journal of Petroleum Technology*, bd. 25, nr. 03, s. 339–353, mar. 1973, doi: 10.2118/3544-PA.

[73] O. Vazquez, «Scale Inhibitor Squeeze Treatments», i *Modelling Oilfield Scale Squeeze Treatments : From Core to Reservoir*, O. Vazquez, Red., Cham: Springer International Publishing, 2023, s. 57–71. doi: 10.1007/978-3-319-71852-1_4.

[74] J. R. Griffin, J. R. Johnstone, T. E. Cotter, og A. E. O'Brien, «Factors Affecting the Stability of Scale Inhibitors Used for Capillary Injection in High Temperature Wells», presentert på SPE International Symposium on Oilfield Chemistry, OnePetro, apr. 2013. doi: 10.2118/164128-MS.

[75] K. R. Rosa, M. C. Bezerra, R. A. Fontes, E. A. Ponzio, og A. A. Rocha, «Study of Thermal Stability of Scale Inhibitors and its Impact on Processing Plants», presentert på SPE International Oilfield Scale Conference and Exhibition, OnePetro, mai 2016. doi: 10.2118/179907-MS.

[76] L. A. Bromley, D. Cottier, R. J. Davey, B. Dobbs, S. Smith, og B. R. Heywood, «Interactions at the organic/inorganic interface: molecular design of crystallization inhibitors for barite», *Langmuir*, bd. 9, nr. 12, s. 3594–3599, des. 1993, doi: 10.1021/la00036a040.

[77] M. F. Mady, A. H. Karaly, S. Abdel-Azeim, I. A. Hussein, M. A. Kelland, og A. Younis, «Phosphonated Lower-Molecular-Weight Polyethyleneimines as Oilfield Scale Inhibitors: An Experimental and Theoretical Study», *Ind. Eng. Chem. Res.*, bd. 61, nr. 27, s. 9586–9599, jul. 2022, doi: 10.1021/acs.iecr.2c01730.

[78] M. F. Mady, A. Bagi, og M. A. Kelland, «Synthesis and Evaluation of New Bisphosphonates as Inhibitors for Oilfield Carbonate and Sulfate Scale Control», *Energy Fuels*, bd. 30, nr. 11, s. 9329–9338, nov. 2016, doi: 10.1021/acs.energyfuels.6b02117.

[79] Z. Amjad, «Inhibition of Barium Sulfate Precipitation: Effects of Additives, Solution

pH, and Supersaturation», i *Water Treatment*, 1994, s. 47–56. [Online]. Tilgjengelig på:
<https://www.lubrizol.com/-/media/F060655BD24D4023A19F16F2D441CACD.pdf>

[80] D. W. Griffiths, S. D. Roberts, og S.-T. Liu, «Inhibition Of Calcium Sulfate Dihydrate Crystal Growth By Phosphonic Acids - Influence Of Inhibitor Structure And Solution Ph», presentert på SPE Oilfield and Geothermal Chemistry Symposium, OnePetro, jan. 1979. doi: 10.2118/7862-MS.

Appendix

A-1 NMR Spectra

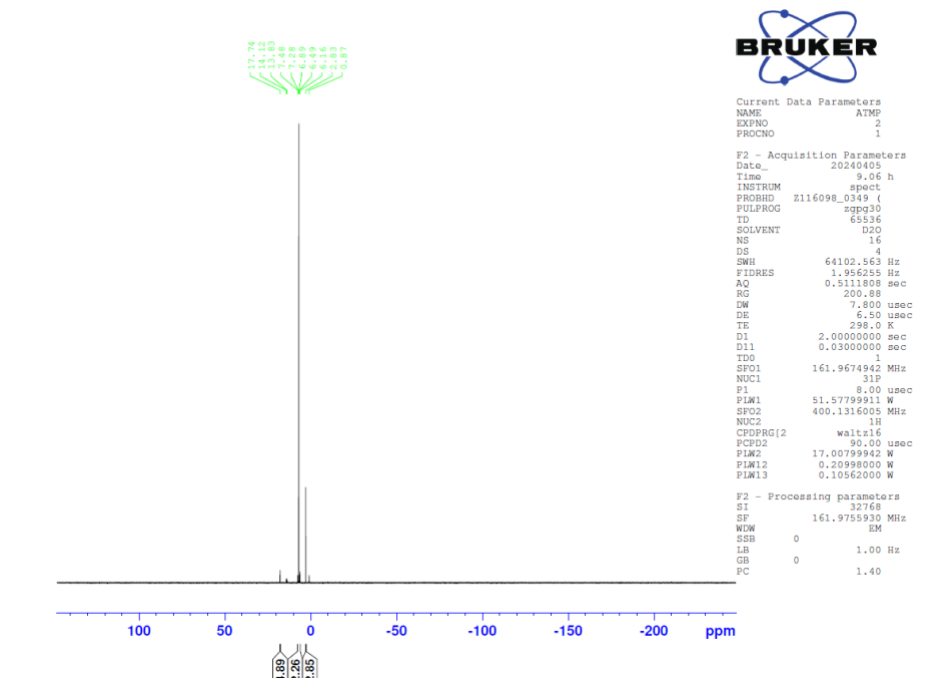


Figure A-1.1 NMR spectrum of ATMP.

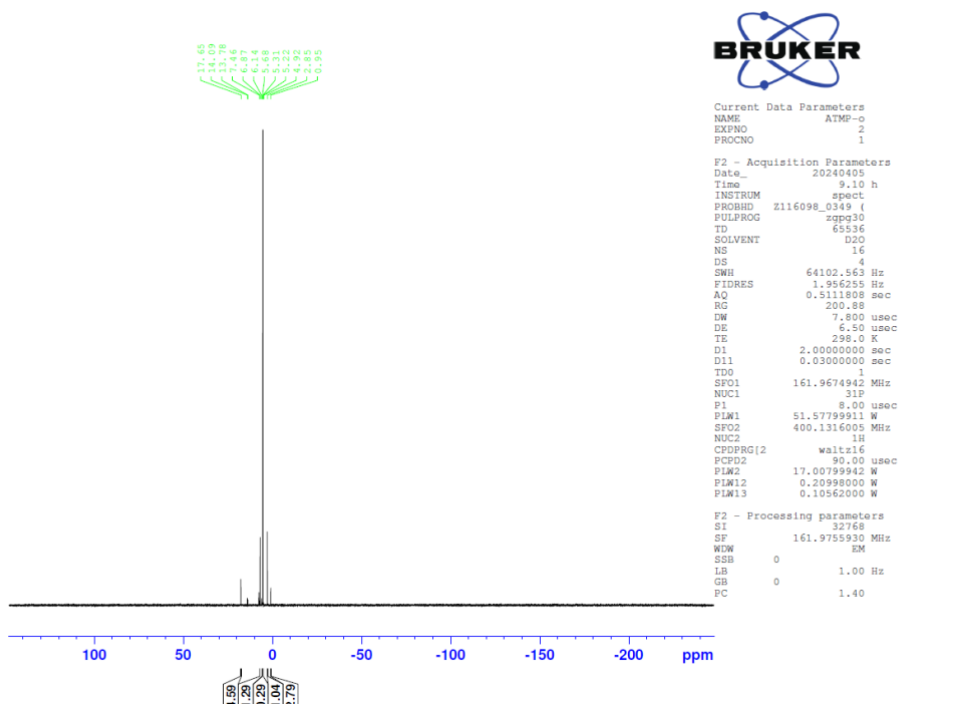


Figure A-1.2 NMR spectrum of ATMP-O.

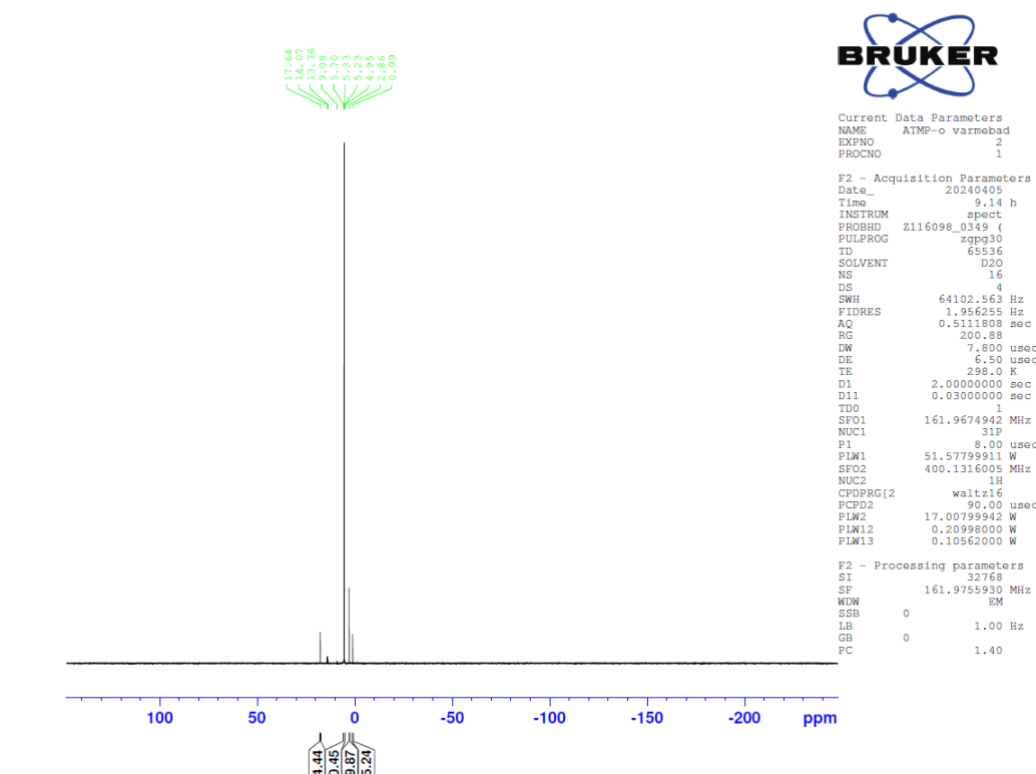


Figure A-1.3 NMR spectrum of ATMP-O after oxidation in heat bath.

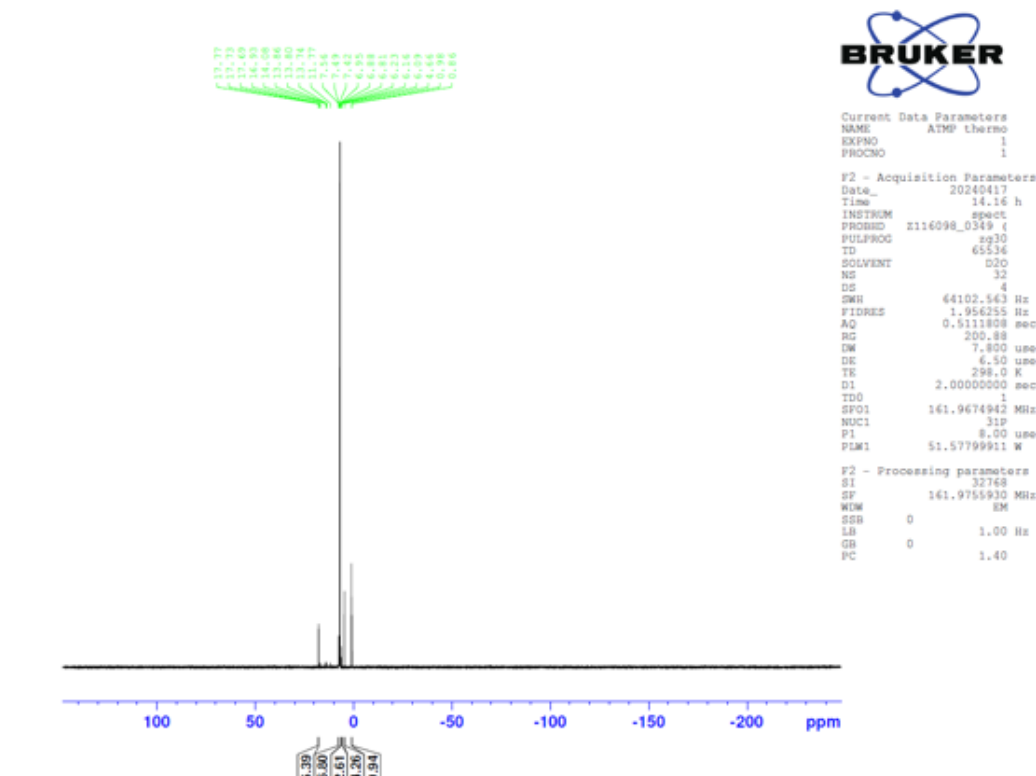


Figure A-1.4 NMR spectrum of ATMP after thermal aging at 140 °C.

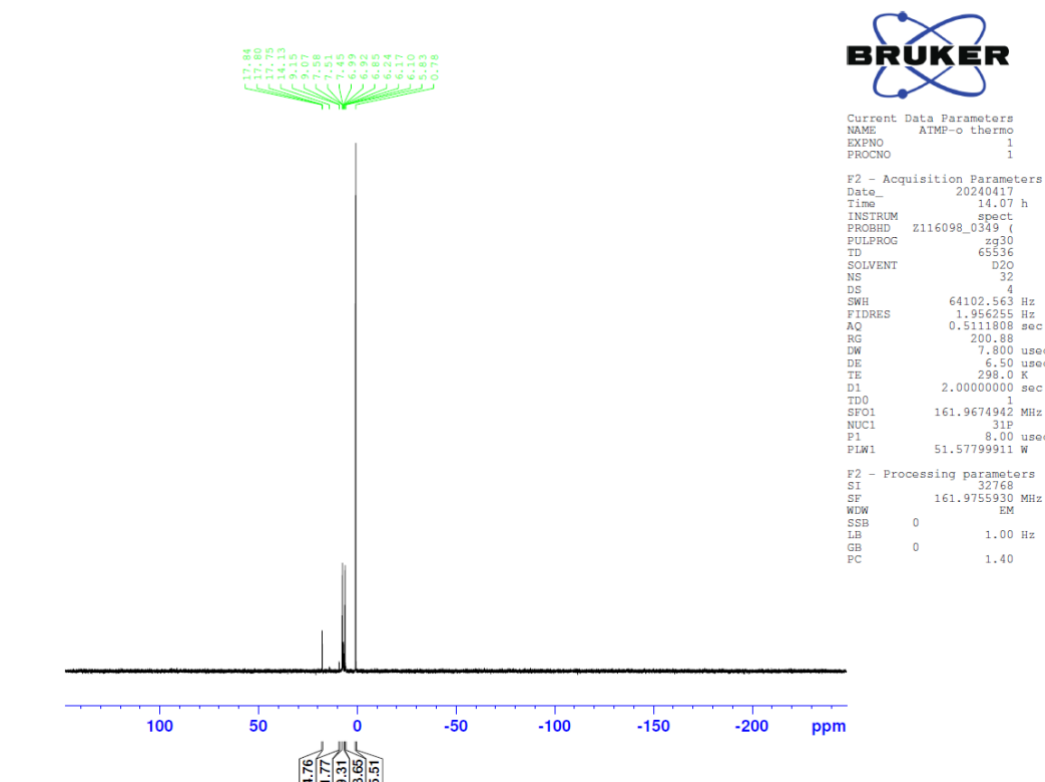


Figure A-1.5 NMR spectrum of ATMP-O after thermal aging at 140 °C.

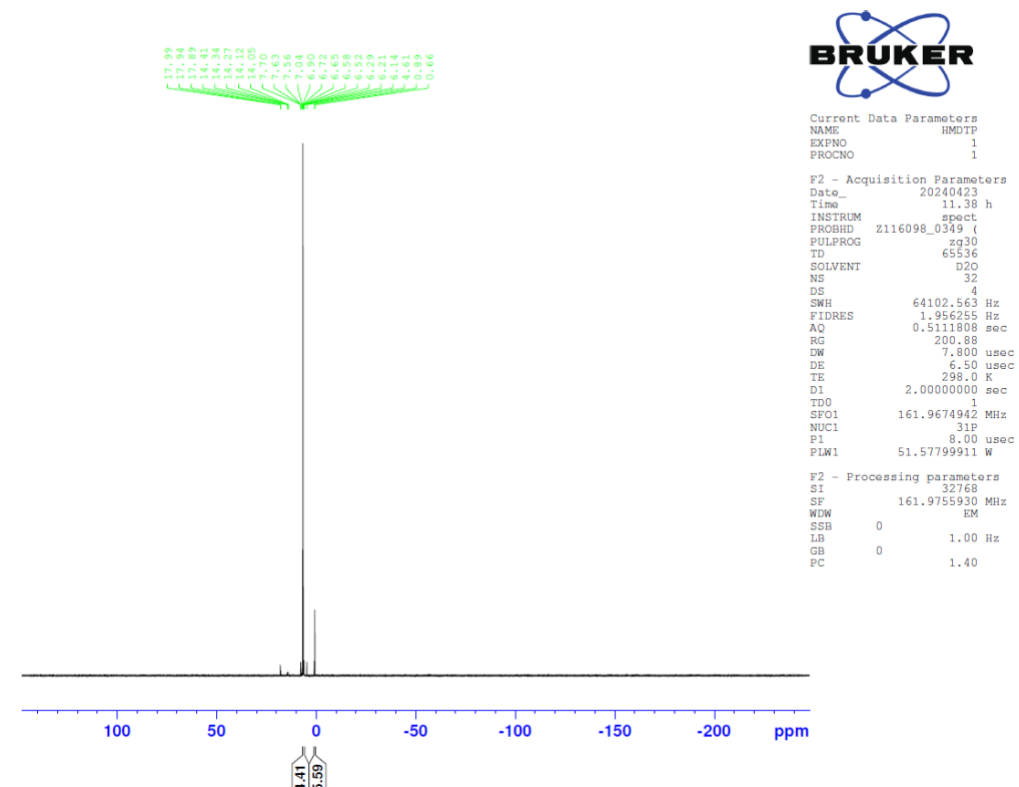


Figure A-1.6 NMR spectrum of HMDTP.

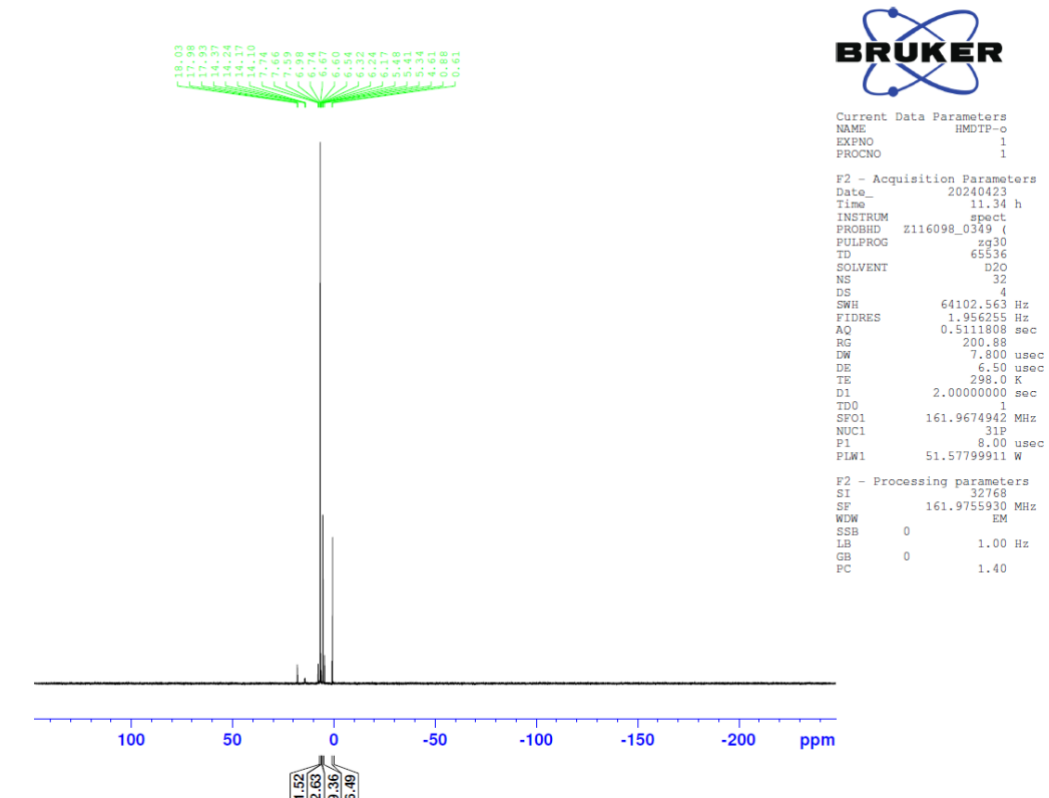


Figure A-1.7 NMR spectrum of HMDTP-O.

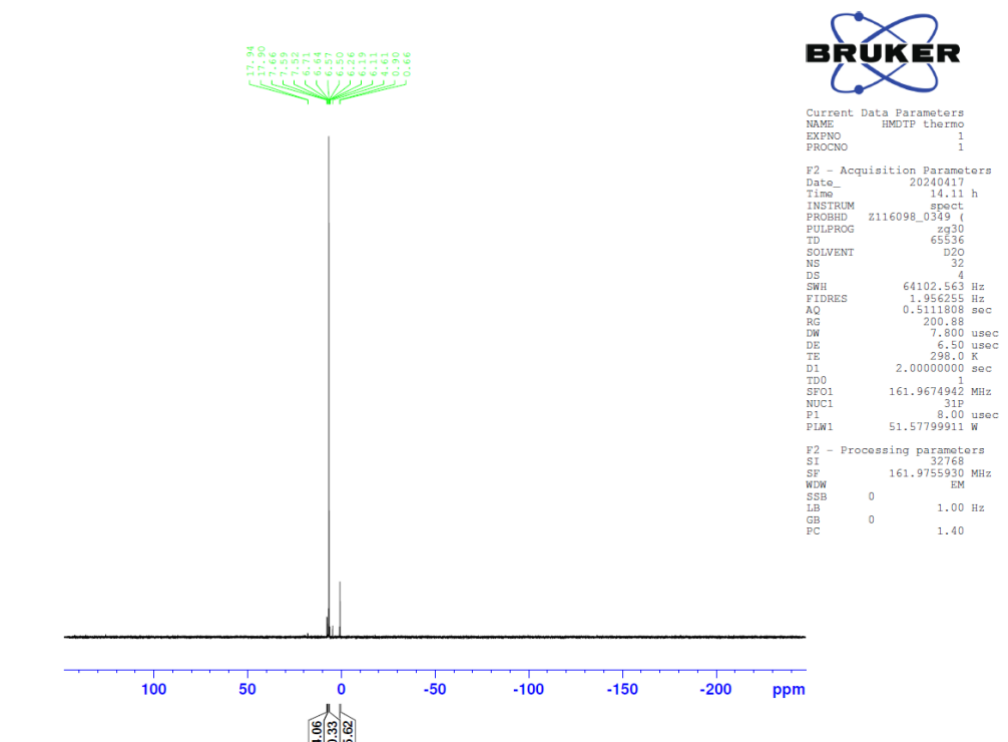


Figure A-1.8 NMR spectrum of HMDTP after thermal aging at 140 °C.

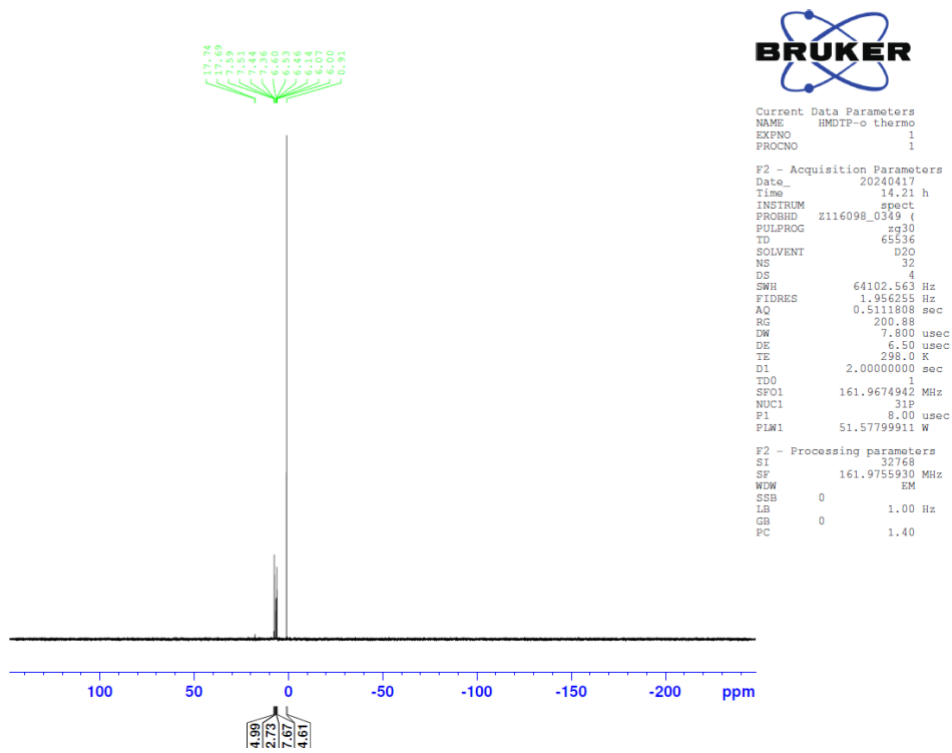


Figure A-1.9 NMR spectrum of HMDTP-O after thermal aging at 140 °C.

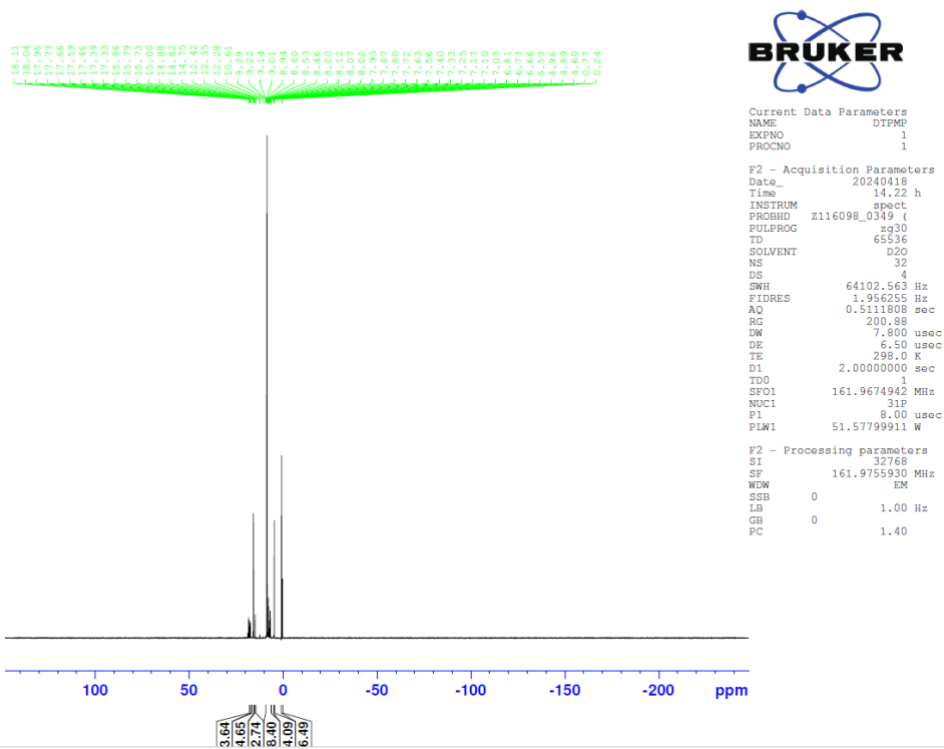


Figure A-1.10 NMR spectrum of DTPMP.

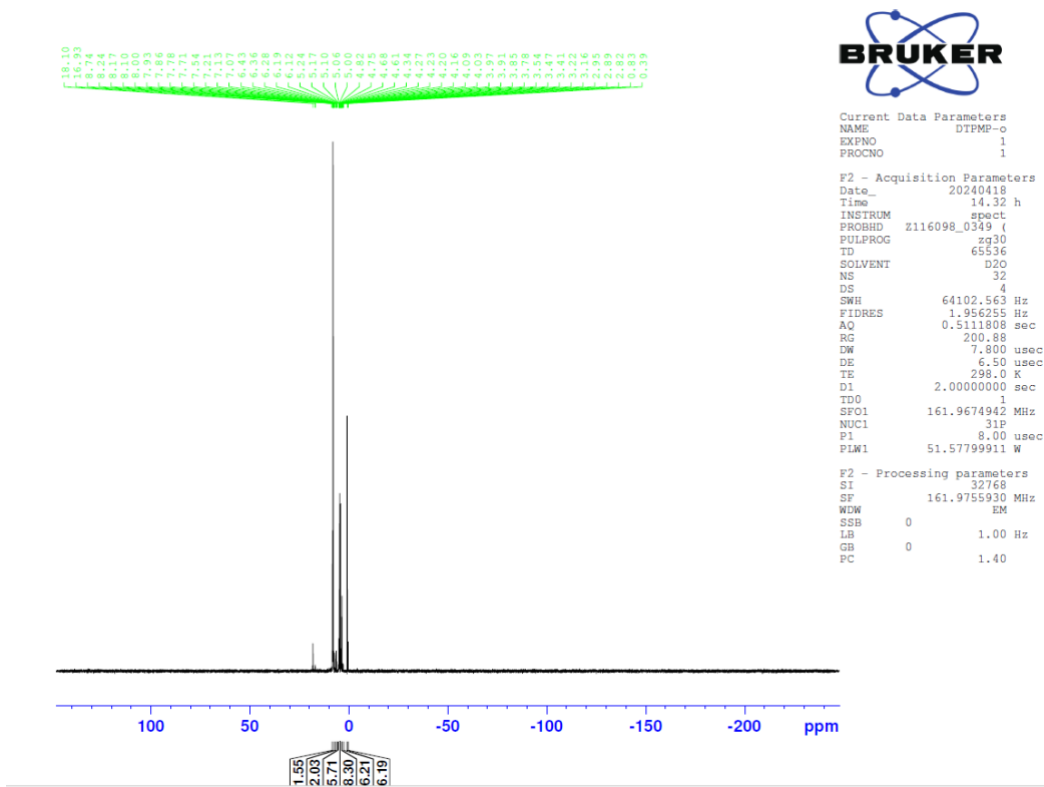


Figure A-1.11 NMR spectrum of DTPMP-O.

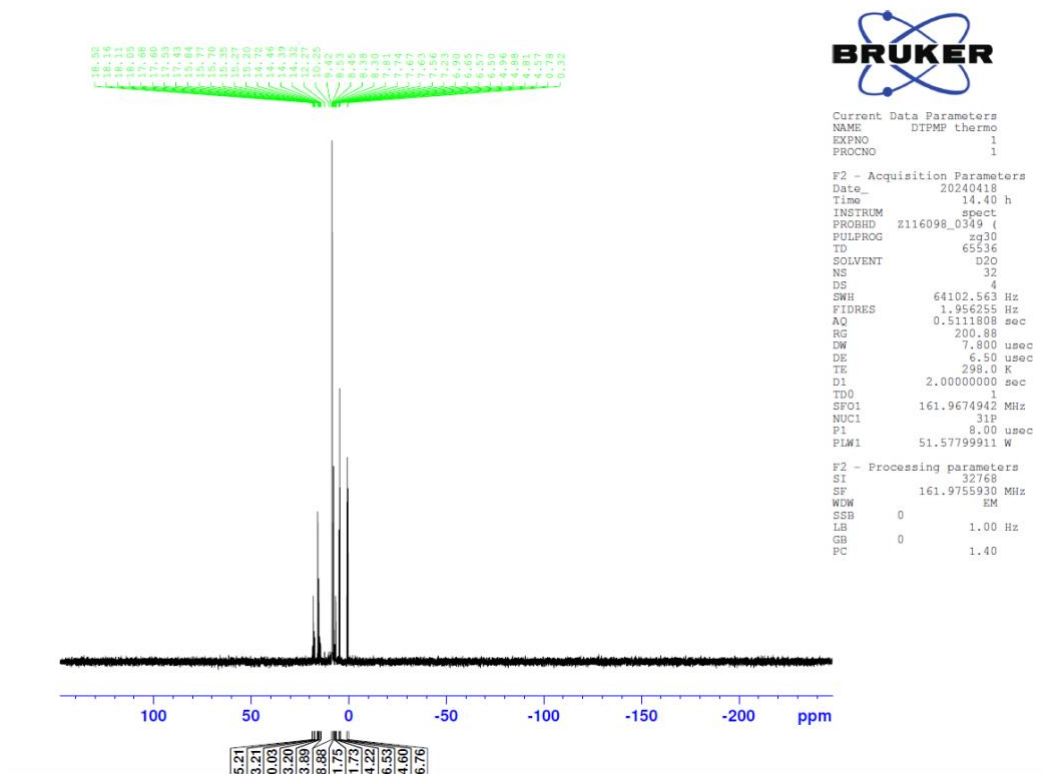


Figure A-1.12 NMR spectrum of DTPMP after thermal aging at 140 °C.

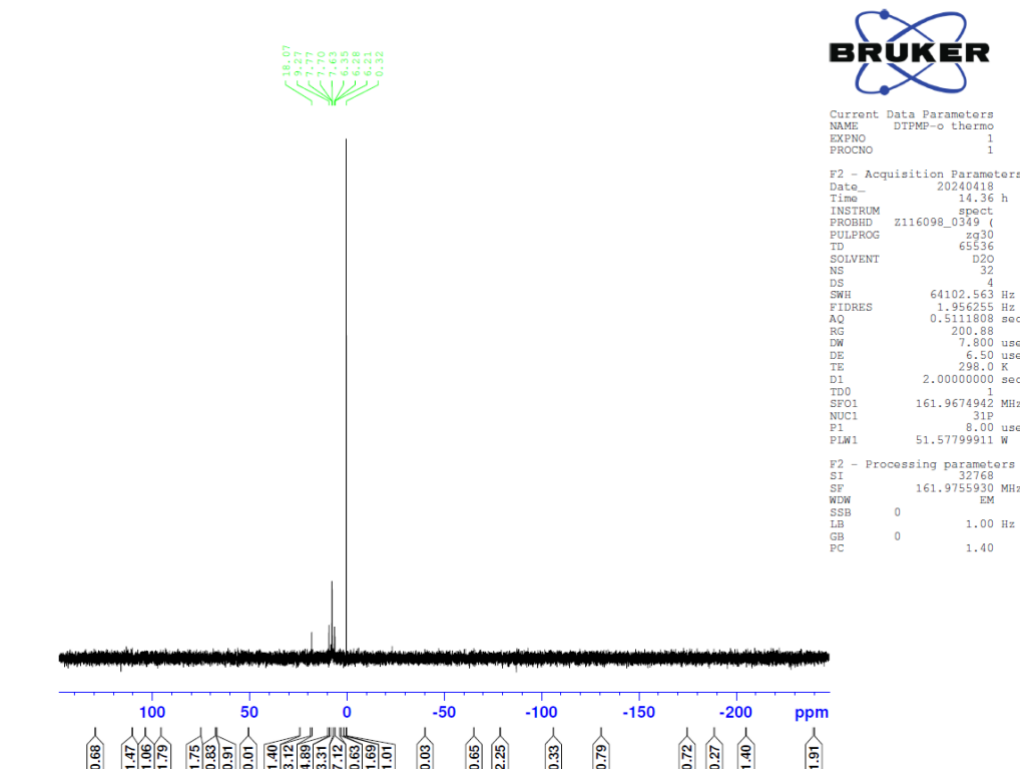


Figure A-1.13 NMR spectrum of DTPMP-O after thermal aging at 140 °C.

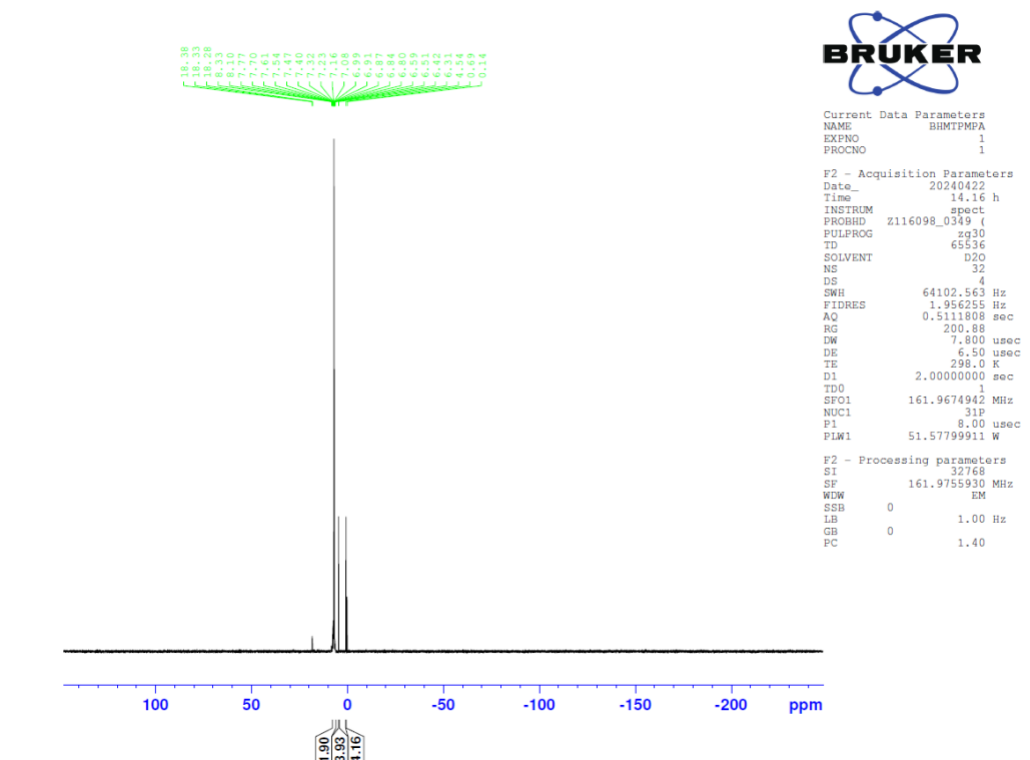


Figure A-1.14 NMR spectrum of BHMTMPMA.

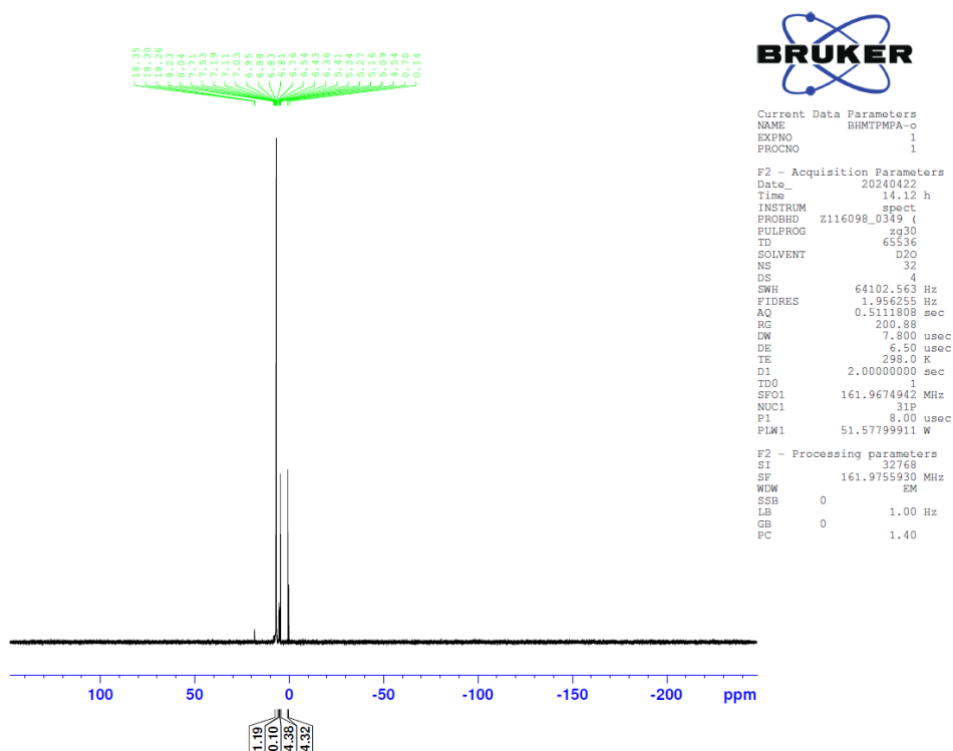


Figure A-1.15 NMR spectrum of BHMTMPMA-O.

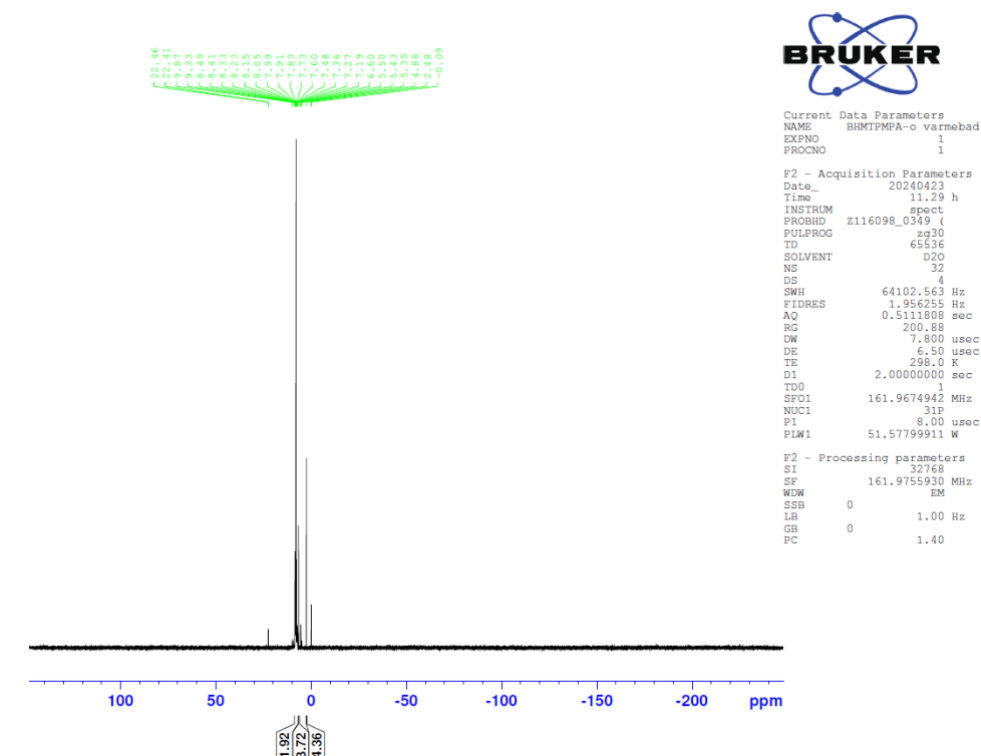


Figure A-1.16 NMR spectrum of BHMTMPMA-O after oxidation in heat bath.

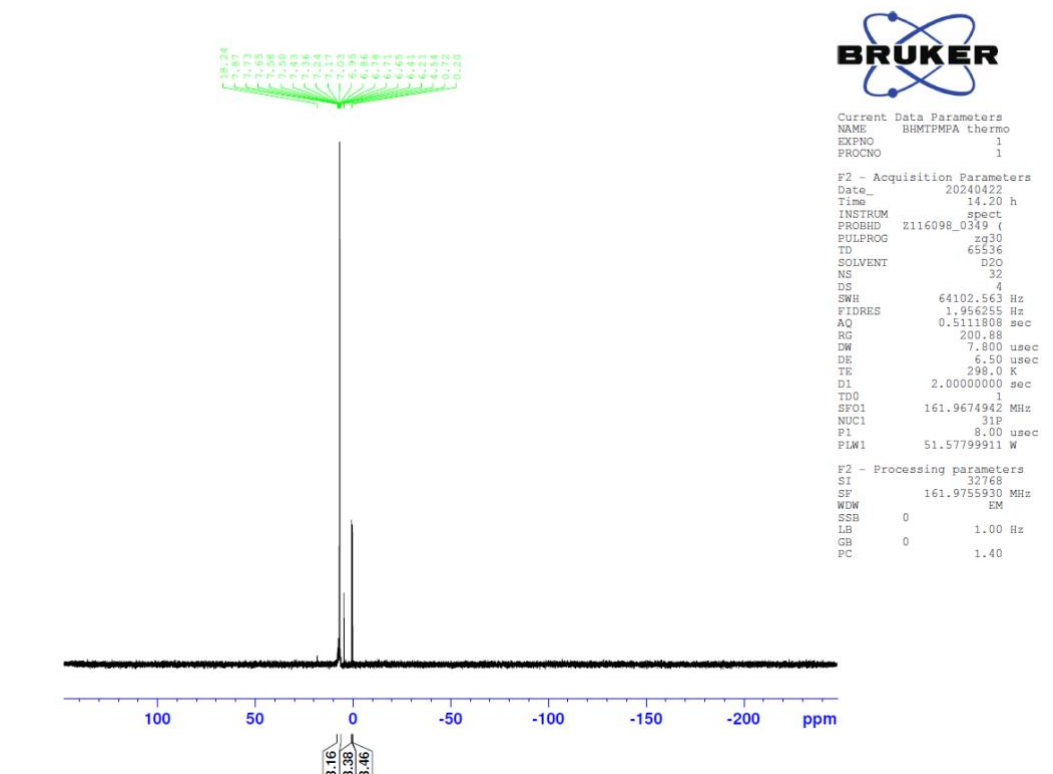


Figure A-1.17 NMR spectrum of BHMTMPA after thermal aging at 140 °C.

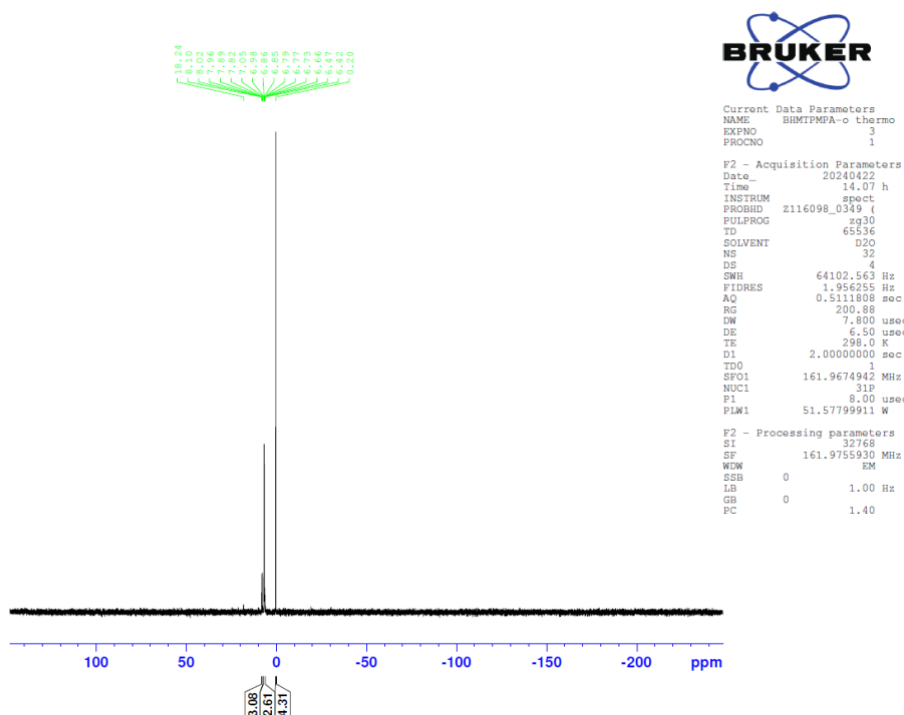


Figure A-1.18 NMR spectrum of BHMTMPA-O after thermal aging at 140 °C.

A-2 High-Pressure Dynamic Tube Blocking Rig Test Results

Table A-2.1 FIC and time results from the tests on the high-pressure dynamic tube blocking rig.

Scale Inhibitor	pH (1000ppm)	Calcite		Barite	
		FIC conc. (ppm)	Time (min)	FIC conc. (ppm)	Time (min)
ATMP (pH 2)	2-3	1	7-12	100	14
ATMP-o (pH 2)	2	2	44-52	100	13
ATMP (pH 6)	6	1	11	20	29-30
ATMP (pH 6) thermo 140	6	1 and 2	6 and 56	20	49-55
ATMP (pH 6) thermo 160	6	1	19-24	20	39
ATMP-o (pH 6)	6	2	28-35	20	4
ATMP-o (pH 6) varmebad	6	2	6-22	50	42-45
ATMP-o (pH 6) thermo 140	6	2	6-19	50	40-41
ATMP-o (pH 6) thermo 160	6	2	14-30	50	32-35
ATMP-o (pH 6) varmebad thermo	6	1	9-15	20	13-14
ATMP (pH 10)	7-8	<1	-	10	10-18
ATMP-o (pH 10)	7-8	<1	-	10	7-11
ATMP-o (AQUACID) (pH 10-11)	8	2	8-22	20	11-13
HMDTP (pH 6-7)	6	<1	-	10	17 - 21
HMDTP (pH 6-7) thermo 140	6	<1	-	5	5-9
HMDTP (pH 6-7) thermo 160	6	<1	-	10	53-59
HMDTP-o (pH 6-7)	6	<1	-	20	34
HMDTP-o (pH 6-7) thermo 140	6	2	13-27	20	1-3
HMDTP-o (pH 6-7) thermo 160	6	2	8-28	20	1-2
DTPMP (pH 1-2)	3	2	15-25	100	48
DTPMP-o (pH 1-2)	3	2	26	50	15-17
DTPMP (pH 6)	6	2	26	10	25-26
DTPMP (pH 6) thermo 140	6	2	23-25	10	18
DTPMP (pH 6) thermo 160	6	1	8	20	20
DTPMP-o (pH 6)	6	2	13-25	10	8-11
DTPMP-o (pH 6) thermo 140	6	2	10-22	50	25-26
DTPMP-o (pH 6) thermo 160	6	2	14-25	50	10-16

DTPMP-o (pH 6 a.b.ox.)	6	2	10-21	20	17
BHMTPMPA (pH 1-2)	2	1	9-24	100	11
BHMTPMPA-o (pH 1-2)	2	2	31-36	100	10
BHMTPMPA (pH 6)	6	1 and 2	8 and 50	5	9-10
BHMTPMPA (pH 6) thermo 140	6	1	30-35	10	18-23
BHMTPMPA (pH 6) thermo 160	6	1	10-19	10	14-19
BHMTPMPA-o (pH 6)	6	2	21-30	10	47-52
BHMTPMPA-o (pH 6) thermo 140	6	2	11-25	20 and 10	1 and 51
BHMTPMPA-o (pH 6) thermo 160	5	2	14-23	10 and 20	3 and 42
BHMTPMPA-o (pH 6 a.b.ox.)	5	2	19-23	10	2-4

A-3 Calcium Compatibility Test Results

This chapter contains our interpretation of all calcium compatibility tests.

ATMP (pH 2-3)

Table A-3.1 100 ppm of Ca²⁺ and 30 000 ppm of NaCl for ATMP (pH 2-3).

Dose (ppm)	Appearance					
	At mixing	30 min	1 h	2 h	4 h	24 h
100	Clear	Clear	Clear	Clear	Clear	Clear
1000	Clear	Clear	Clear	Clear	Clear	Clear
10000	Clear	Clear	Clear	Clear	Clear	Clear
50000	Clear	Clear	Clear	Clear	Clear	Clear

Table A-3.2 1 000 ppm of Ca²⁺ and 30 000 ppm of NaCl for ATMP (pH 2-3).

Dose (ppm)	Appearance					
	At mixing	30 min	1 h	2 h	4 h	24 h
100	Clear	Clear	Clear	Clear	Clear	Clear
1000	Clear	Clear	Clear	Clear	Clear	Clear
10000	Clear	Clear	Clear	Clear	Clear	Clear
50000	Clear	Clear	Clear	Clear	Clear	Clear

Table A-3.3 10 000 ppm of Ca²⁺ and 30 000 ppm of NaCl for ATMP (pH 2-3).

Dose (ppm)	Appearance					
	At mixing	30 min	1 h	2 h	4 h	24 h
100	Clear	Clear	Clear	Clear	Clear	Clear
1000	Clear	Clear	Clear	Clear	Clear	Clear
10000	Clear	Clear	Clear	Clear	Clear	Clear
50000	Clear	Clear	Little precipitation (looks like snow flakes)	Precipitation (crystals stuck on the bottom)	Precipitation (crystals stuck on the bottom)	Precipitation (crystals stuck on the bottom)

ATMP-O (pH 2)

Table A-3.4 100 ppm of Ca²⁺ and 30 000 ppm of NaCl for ATMP-O (pH 2).

Dose (ppm)	Appearance					
	At mixing	30 min	1 h	2 h	4 h	24 h
100	Clear	Clear	Clear	Clear	Clear	Clear
1000	Clear	Clear	Clear	Clear	Clear	Clear
10000	Clear	Clear	Clear	Clear	Clear	Clear
50000	Clear	Clear	Clear	Clear	Clear	Clear

Table A-3.5 1 000 ppm of Ca²⁺ and 30 000 ppm of NaCl for ATMP-O (pH 2).

Dose (ppm)	Appearance					
	At mixing	30 min	1 h	2 h	4 h	24 h
100	Clear	Clear	Clear	Clear	Clear	Clear
1000	Clear	Clear	Clear	Clear	Clear	Clear
10000	Clear	Clear	Clear	Clear	Clear	Clear
50000	Clear	Clear	Clear	Clear	Clear	Clear

Table A-3.6 10 000 ppm of Ca²⁺ and 30 000 ppm of NaCl for ATMP-O (pH 2).

Dose (ppm)	Appearance					
	At mixing	30 min	1 h	2 h	4 h	24 h
100	Clear	Clear	Clear	Clear	Clear	Clear
1000	Clear	Clear	Clear	Clear	Clear	Clear
10000	Clear	Clear	Clear	Clear	Clear	Clear
50000	Clear	Clear	Clear	Clear	Clear	Clear

ATMP (pH 6)

Table A-3.7 100 ppm of Ca²⁺ and 30 000 ppm of NaCl for ATMP (pH 6).

Dose (ppm)	Appearance					
	At mixing	30 min	1 h	2 h	4 h	24 h
100	Clear	Clear	Clear	Clear	Clear	Clear
1000	Clear	Clear	Clear	Clear	Clear	Clear
10000	Clear	Clear	Clear	Clear	Clear	Clear
50000	Clear	Clear	Clear	Clear	Clear	Clear

Table A-3.8 1 000 ppm of Ca²⁺ and 30 000 ppm of NaCl for ATMP (pH 6).

Dose (ppm)	Appearance					
	At mixing	30 min	1 h	2 h	4 h	24 h
100	Clear	Clear	Clear	Clear	Clear	Clear
1000	Very slight haze	Haze	Slight haze/ precipitated	Haze/ precipitated	Haze/ precipitated	Haze/ precipitated
10000	Haze	Very haze	Haze/ precipitated	Haze/ precipitated	Haze/ precipitated	Haze/ precipitated
50000	Clear	Clear	Clear	Clear	A bit precipitation	Haze/ precipitated

Table A-3.9 10 000 ppm of Ca²⁺ and 30 000 ppm of NaCl for ATMP (pH 6).

Dose (ppm)	Appearance					
	At mixing	30 min	1 h	2 h	4 h	24 h
100	Clear	Clear	Very slight haze	Very slight haze	Very slight haze	Very slight haze
1000	Slight haze	Slight haze	Slight haze	Slight haze	Slight haze	Slight haze
10000	Haze	Very haze	Very haze	Very haze	Very haze	Very haze
50000	Precipitated haze	Precipitated	Very precipitated	Very precipitated	Very precipitated	100% precipitated

ATMP-O (pH 6)

Table A-3.10 100 ppm of Ca²⁺ and 30 000 ppm of NaCl for ATMP-O (pH 6).

Dose (ppm)	Appearance					
	At mixing	30 min	1 h	2 h	4 h	24 h
100	Clear	Clear	Clear	Clear	Clear	Clear
1000	Clear	Clear	Very little haze	Slight haze	Slight haze	Slight haze
10000	Clear	Clear	Clear	Clear	Slight haze	Haze
50000	Clear	Clear	Clear	Clear	Clear	Haze

Table A-3.11 1 000 ppm of Ca²⁺ and 30 000 ppm of NaCl for ATMP-O (pH 6).

Dose (ppm)	Appearance					
	At mixing	30 min	1 h	2 h	4 h	24 h
100	Clear	Clear	Very little haze	Very little haze	Very little haze	Very little haze
1000	Clear	Haze	Haze/precipitated	Precipitated	Precipitated	Haze/precipitated
10000	Haze	Very haze	Very haze/precipitated	Very haze/precipitated	Very haze/precipitated	Very haze/precipitated
50000	Clear	Haze	Very haze/precipitated	Very haze	Very haze	Very haze

Table A-3.12 10 000 ppm of Ca²⁺ and 30 000 ppm of NaCl for ATMP-O (pH 6).

Dose (ppm)	Appearance					
	At mixing	30 min	1 h	2 h	4 h	24 h
100	Clear	Very little haze	Slight haze	Slight precipitation	Slight precipitation	Slight precipitation
1000	Very little haze	Slight haze/precipitated	Haze/precipitated	Precipitated	Precipitated	Precipitated
10000	Haze	Haze/precipitated	Haze/precipitated	Haze/precipitated	Haze/precipitated gel-ish	Haze/precipitated gel-ish
50000	Precipitated	Thick precipitation	Almost solid gel	Solid gel (gets liquid when shaken)	Solid gel	Solid

ATMP (pH 7-8)

Table A-3.13 100 ppm of Ca²⁺ and 30 000 ppm of NaCl for ATMP (pH 7-8).

Dose (ppm)	Appearance					
	At mixing	30 min	1 h	2 h	4 h	24 h
100	Clear	Clear	Clear	Clear	Clear (very little prec)	Clear (very little prec)
1000	Clear	Clear	Clear	Clear	Clear (very little prec)	Clear (some prec)
10000	Clear	Clear	Clear	Clear	Clear (very little prec)	Clear (very little prec)
50000	Clear	Clear	Clear	Clear	Clear (very little prec)	Clear (very little prec)

Table A-3.14 1 000 ppm of Ca²⁺ and 30 000 ppm of NaCl for ATMP (pH 7-8).

Dose (ppm)	Appearance					
	At mixing	30 min	1 h	2 h	4 h	24 h
100	Clear	Slight haze	Slight haze	Slight haze	Slight haze	Slight haze
1000	Slight haze	Haze (a bit clumpy)	Haze (a bit clumpy)	Haze (a bit clumpy)	Haze (a bit clumpy)	Haze (a bit clumpy)
10000	Clear	Clear	Slight haze	Slight haze	Slight haze	Precipitated
50000	Clear	Clear	Clear	Clear	Clear	Clear

Table A-3.15 10 000 ppm of Ca²⁺ and 30 000 ppm of NaCl for ATMP (pH 7-8).

Dose (ppm)	Appearance					
	At mixing	30 min	1 h	2 h	4 h	24 h
100	Clear	Slight haze	Slight haze	Slight haze	Slight haze	Slight haze
1000	Slight haze	Slight haze	Slight haze	Slight haze	Slight haze	Slight haze (little precipitate)
10000	Thick precipitate	Thick haze/precipitate	Thick haze/precipitate	Thick haze/precipitate	Thick haze/precipitate	Thick haze/precipitate
50000	Very thick precipitate	Very thick precipitate	Very thick precipitate	Very thick precipitate	Very thick precipitate	Very thick precipitate

ATMP-O (pH 7-8)

Table A-3.16 100 ppm of Ca²⁺ and 30 000 ppm of NaCl for ATMP-O (pH 7-8).

Dose (ppm)	Appearance					
	At mixing	30 min	1 h	2 h	4 h	24 h
100	Clear	Clear	Clear (very little prec)	Clear (very little prec)	Clear (very little prec)	Clear (little prec)
1000	Clear	Clear	Clear (very little prec)	Clear (very little prec)	Clear (little prec)	Slight precipitate
10000	Clear	Clear	Clear	Clear	Clear	Clear
50000	Clear	Clear	Clear	Clear	Clear	Clear

Table A-3.17 1 000 ppm of Ca²⁺ and 30 000 ppm of NaCl for ATMP-O (pH 7-8).

Dose (ppm)	Appearance					
	At mixing	30 min	1 h	2 h	4 h	24 h
100	Clear	Slight haze	Slight haze	Slight haze	Slight haze	Slight haze
1000	Haze	Haze	Haze	Haze	Haze	Haze
10000	Clear	Haze (but a little less than the above)	Haze (but a little less than the above)	Haze (but a little less than the above)	Haze (but a little less than the above)	Haze
50000	Clear	Clear	Clear	Clear	Clear	Haze (some more than the two above)

Table A-3.18 10 000 ppm of Ca²⁺ and 30 000 ppm of NaCl for ATMP-O (pH 7-8).

Dose (ppm)	Appearance					
	At mixing	30 min	1 h	2 h	4 h	24 h
100	Clear	Slight haze/ Precipitated	Slight haze/ precipitated	Slight haze/ precipitated	Slight haze/ precipitated	Slight haze/ precipitated
1000	Slight haze	Slight haze	Slight haze	Slight haze	Slight haze	Slight haze
10000	Thick haze	Thick haze	Thick haze	Thick haze	Thick haze	Thick haze + some precipitation
50000	Precipitated	Precipitated	Thick precipitation	Thick precipitation	Thick precipitation	Thick precipitation + haze

ATMP-O (AQUACID pH 8)

Table A-3.19 100 ppm of Ca²⁺ and 30 000 ppm of NaCl for ATMP-O (AQUACID pH 8).

Dose (ppm)	Appearance					
	At mixing	30 min	1 h	2 h	4 h	24 h
100	Clear	Clear	Clear	Clear	Slight precipitate	Slight precipitate
1000	Clear	Slight haze	Slight haze	Slight haze	Slight haze	Slight haze
10000	Clear	Clear	Clear	Clear	Clear	Clear
50000	Clear	Clear	Clear	Clear	Clear	Clear

Table A-3.20 1 000 ppm of Ca²⁺ and 30 000 ppm of NaCl for ATMP-O (AQUACID pH 8).

Dose (ppm)	Appearance					
	At mixing	30 min	1 h	2 h	4 h	24 h
100	Clear	Slight haze/precipitate	Slight haze/precipitate	Slight haze/precipitate	Slight haze/precipitate	Slight haze/precipitate
1000	Haze	Haze	Haze	Haze	Haze	Haze
10000	Haze	Haze	Haze	Haze	Haze	Haze
50000	Clear	Clear	Clear	Clear	Clear	Clear

Table A-3.21 10 000 ppm of Ca²⁺ and 30 000 ppm of NaCl for ATMP-O (AQUACID pH 8).

Dose (ppm)	Appearance					
	At mixing	30 min	1 h	2 h	4 h	24 h
100	Clear	Slight haze/precipitated	Slight haze/precipitated	Slight haze/precipitated	Slight haze/precipitated	Slight haze/precipitated
1000	Haze	Haze	Haze	Haze	Haze	Haze
10000	Thick haze	Thick haze	Viscous haze	Viscous haze	Viscous haze	Viscous haze
50000	Precipitated	Precipitated	Precipitated	Very viscous (thick) precipitated	Even more viscous (thick) precipitated	Even more viscous (thick)

HMDTP (pH 6)

Table A-3.22 100 ppm of Ca²⁺ and 30 000 ppm of NaCl for HMDTP (pH 6).

Dose (ppm)	Appearance					
	At mixing	30 min	1 h	2 h	4 h	24 h
100	Clear	Clear	Clear	Clear	Clear	Clear
1000	Clear	Clear	Clear	Clear	Clear	Clear
10000	Clear	Clear	Clear	Clear	Clear	Clear
50000	Clear	Clear	Clear	Clear	Clear	Clear

Table A-3.23 1 000 ppm of Ca²⁺ and 30 000 ppm of NaCl for HMDTP (pH 6).

Dose (ppm)	Appearance					
	At mixing	30 min	1 h	2 h	4 h	24 h
100	Clear	Clear	Clear	Clear	Clear	Clear
1000	Clear	Haze	Haze	Haze	Slight particulate haze	Slight particulate haze
10000	Clear	Precipitation /haze	Precipitation /haze	Precipitation /haze	Particulate haze	Particulate haze
50000	Clear	Clear	Clear	Clear	Clear	Clear

Table A-3.24 10 000 ppm of Ca²⁺ and 30 000 ppm of NaCl for HMDTP (pH 6).

Dose (ppm)	Appearance					
	At mixing	30 min	1 h	2 h	4 h	24 h
100	Clear	Clear	Clear	Clear	Clear	Clear
1000	Clear	Haze	Haze	Haze/a bit precipitated	Particulate haze	Particulate haze
10000	Precipitation	Precipitation	Precipitation	Precipitation	Precipitation	Precipitation
50000	Very thick and clumpy precipitation	Very thick and clumpy precipitation	Very thick and clumpy precipitation	Very thick and clumpy precipitation	Very thick and clumpy precipitation	Very thick and clumpy precipitation

HMDTP-O (pH 6)

Table A-3.25 100 ppm of Ca²⁺ and 30 000 ppm of NaCl for HMDTP-O (pH 6).

Dose (ppm)	Appearance					
	At mixing	30 min	1 h	2 h	4 h	24 h
100	Clear	Clear	Clear	Clear	Clear	Clear
1000	Clear	Clear	Clear	Clear	Clear	Clear
10000	Clear	Clear	Clear	Clear	Clear	Clear
50000	Clear	Clear	Clear	Clear	Clear	Clear

Table A-3.26 1 000 ppm of Ca²⁺ and 30 000 ppm of NaCl for HMDTP-O (pH 6).

Dose (ppm)	Appearance					
	At mixing	30 min	1 h	2 h	4 h	24 h
100	Clear	Clear	Clear	Clear	Clear	Clear
1000	Clear	Clear	Clear	Clear	Slight haze	Slight haze (bottom)
10000	Clear	Haze	Haze/precipitation	Haze/precipitation	Haze/precipitation	More haze/precipitation
50000	Clear	Clear	Clear	Clear	Clear	Clear

Table A-3.27 10 000 ppm of Ca²⁺ and 30 000 ppm of NaCl for HMDTP-O (pH 6).

Dose (ppm)	Appearance					
	At mixing	30 min	1 h	2 h	4 h	24 h
100	Clear	Clear	Clear	Clear	Clear	Clear
1000	Clear	Haze	Haze	Haze/litte precipitated	Haze/precipitated	Haze/precipitated
10000	Haze	Very haze	Very haze	Very haze/some precipitate	Very haze/some precipitate	Very haze/some precipitate
50000	Precipitation	Thick, almost solid precipitation	Thick, almost solid precipitation	Thick, almost solid precipitation	Thick precipitation	Thick precipitation

DTPMP (pH 3)

Table A-3.28 100 ppm of Ca²⁺ and 30 000 ppm of NaCl for DTPMP (pH 3).

Dose (ppm)	Appearance					
	At mixing	30 min	1 h	2 h	4 h	24 h
100	Clear	Clear	Clear	Clear	Clear	Clear
1000	Clear	Clear	Clear	Clear	Clear	Clear
10000	Clear	Clear	Clear	Clear	Clear	Clear
50000	Clear	Clear	Clear	Clear	Clear	Clear

Table A-3.29 1 000 ppm of Ca²⁺ and 30 000 ppm of NaCl for DTPMP (pH 3).

Dose (ppm)	Appearance					
	At mixing	30 min	1 h	2 h	4 h	24 h
100	Clear	Clear	Clear	Clear	Clear	Clear
1000	Clear	Clear	Clear	Clear	Clear	Clear
10000	Clear	Clear	Clear	Clear	Clear	Clear
50000	Clear	Clear	Clear	Clear	Clear	Clear

Table A-3.30 10 000 ppm of Ca²⁺ and 30 000 ppm of NaCl for DTPMP (pH 3).

Dose (ppm)	Appearance					
	At mixing	30 min	1 h	2 h	4 h	24 h
100	Clear	Clear	Clear	Clear	Clear	Clear
1000	Clear	Clear	Clear	Clear	Clear	Clear
10000	Clear	Clear	Clear	Clear	Clear	Clear
50000	Clear	Clear	Clear	Clear	Clear	Clear

DTPMP-O (pH 3)

Table A-3.31 100 ppm of Ca²⁺ and 30 000 ppm of NaCl for DTPMP-O (pH 3).

Dose (ppm)	Appearance					
	At mixing	30 min	1 h	2 h	4 h	24 h
100	Clear	Clear	Clear	Clear	Clear	Clear
1000	Clear	Clear	Clear	Clear	Clear	Clear
10000	Clear	Clear	Clear	Clear	Clear	Clear
50000	Clear	Clear	Clear	Clear	Clear	Clear

Table A-3.32 1 000 ppm of Ca²⁺ and 30 000 ppm of NaCl for DTPMP-O (pH 3).

Dose (ppm)	Appearance					
	At mixing	30 min	1 h	2 h	4 h	24 h
100	Clear	Clear	Clear	Clear	Clear	Clear
1000	Clear	Clear	Clear	Clear	Clear	Clear
10000	Clear	Clear	Clear	Clear	Clear	Clear
50000	Clear	Clear	Clear	Clear	Clear	Clear

Table A-3.33 10 000 ppm of Ca²⁺ and 30 000 ppm of NaCl for DTPMP-O (pH 3).

Dose (ppm)	Appearance					
	At mixing	30 min	1 h	2 h	4 h	24 h
100	Clear	Clear	Clear	Clear	Clear	Clear
1000	Clear	Clear	Clear	Clear	Clear	Clear
10000	Clear	Clear	Clear	Clear	Clear	Clear
50000	Clear	Clear	Clear	Clear	Clear	Clear

DTPMP (pH 6)

Table A-3.34 100 ppm of Ca²⁺ and 30 000 ppm of NaCl for DTPMP (pH 6).

Dose (ppm)	Appearance					
	At mixing	30 min	1 h	2 h	4 h	24 h
100	Clear	Clear	Clear	Clear	Clear	Clear
1000	Clear	Clear	Clear	Clear	Clear	Clear
10000	Clear	Clear	Clear	Clear	Clear	Clear
50000	Clear	Clear	Clear	Clear	Clear	Clear

Table A-3.35 1 000 ppm of Ca²⁺ and 30 000 ppm of NaCl for DTPMP (pH 6).

Dose (ppm)	Appearance					
	At mixing	30 min	1 h	2 h	4 h	24 h
100	Clear	Clear	Clear	Clear	Clear	Clear
1000	Clear	Clear	Slight haze	Slight haze	Slight haze	Slight precipitate
10000	Clear	Haze	Haze	Haze	Haze	Haze/precipitate
50000	Clear	Clear	Clear	Clear	Clear	Clear

Table A-3.36 10 000 ppm of Ca²⁺ and 30 000 ppm of NaCl for DTPMP (pH 6).

Dose (ppm)	Appearance					
	At mixing	30 min	1 h	2 h	4 h	24 h
100	Clear	Clear	Clear	Clear	Clear	Clear
1000	Clear	Haze	Haze	Haze	Haze/slight precipitation	Haze/slight precipitation
10000	Very haze	Very haze	Very haze	Very haze	Very haze	Very haze
50000	Very haze/precipitate	Very haze/precipitate	Very haze/precipitate	Very haze/precipitate	Very haze/precipitate	Very haze/precipitate

DTPMP-O (pH 6)

Table A-3.37 100 ppm of Ca²⁺ and 30 000 ppm of NaCl for DTPMP-O (pH 6).

Dose (ppm)	Appearance					
	At mixing	30 min	1 h	2 h	4 h	24 h
100	Clear	Clear	Clear	Clear	Clear	Clear
1000	Clear	Clear	Clear	Clear	Clear	Clear
10000	Clear	Clear	Clear	Clear	Clear	Clear
50000	Clear	Clear	Clear	Clear	Clear	Clear

Table A-3.38 1 000 ppm of Ca²⁺ and 30 000 ppm of NaCl for DTPMP-O (pH 6).

Dose (ppm)	Appearance					
	At mixing	30 min	1 h	2 h	4 h	24 h
100	Clear	Clear	Clear	Clear	Clear	Clear
1000	Clear	Slight haze	Slight haze	Slight haze /precipitated	Slight haze /precipitated	Slight haze /precipitated
10000	Very slight haze	Haze	Haze	Haze /precipitated	Haze /precipitated	Haze /precipitated
50000	Clear	Clear	Clear	Clear	Clear	Clear

Table A-3.39 10 000 ppm of Ca²⁺ and 30 000 ppm of NaCl for DTPMP-O (pH 6).

Dose (ppm)	Appearance					
	At mixing	30 min	1 h	2 h	4 h	24 h
100	Clear	Clear	Clear	Clear	Clear	Clear
1000	Haze	Cloudy	Cloudy	Cloudy	Cloudy	Cloudy
10000	Haze /precipitated	Very haze	Very haze	Very haze	Very haze	Very haze
50000	Precipitated	Precipitated	Precipitated	Precipitated	Solid	Solid

BHMTMPMA (pH 2)

Table A-3.40 100 ppm of Ca²⁺ and 30 000 ppm of NaCl for BHMTMPMA (pH 2).

Dose (ppm)	Appearance					
	At mixing	30 min	1 h	2 h	4 h	24 h
100	Clear	Clear	Clear	Clear	Clear	Clear
1000	Clear	Clear	Clear	Clear	Clear	Clear
10000	Clear	Clear	Clear	Clear	Clear	Clear
50000	Clear	Clear	Clear	Clear	Clear	Clear

Table A-3.41 1 000 ppm of Ca²⁺ and 30 000 ppm of NaCl for BHMTMPMA (pH 2).

Dose (ppm)	Appearance					
	At mixing	30 min	1 h	2 h	4 h	24 h
100	Clear	Clear	Clear	Clear	Clear	Clear
1000	Clear	Clear	Clear	Clear	Clear	Clear
10000	Clear	Clear	Clear	Clear	Clear	Clear
50000	Clear	Clear	Clear	Clear	Clear	Clear

Table A-3.42 10 000 ppm of Ca²⁺ and 30 000 ppm of NaCl for BHMTMPMA (pH 2).

Dose (ppm)	Appearance					
	At mixing	30 min	1 h	2 h	4 h	24 h
100	Clear	Clear	Clear	Clear	Clear	Clear
1000	Clear	Clear	Clear	Clear	Clear	Clear
10000	Clear	Clear	Clear	Clear	Clear	Clear
50000	Clear	Clear	Clear	Clear	Clear	Clear

BHMTMPMA-O (pH 2)

Table A-3.43 100 ppm of Ca²⁺ and 30 000 ppm of NaCl for BHMTMPMA-O (pH 2).

Dose (ppm)	Appearance					
	At mixing	30 min	1 h	2 h	4 h	24 h
100	Clear	Clear	Clear	Clear	Clear	Clear
1000	Clear	Clear	Clear	Clear	Clear	Clear
10000	Clear	Clear	Clear	Clear	Clear	Clear
50000	Clear	Clear	Clear	Clear	Clear	Clear

Table A-3.44 1 000 ppm of Ca²⁺ and 30 000 ppm of NaCl for BHMTMPMA-O (pH 2).

Dose (ppm)	Appearance					
	At mixing	30 min	1 h	2 h	4 h	24 h
100	Clear	Clear	Clear	Clear	Clear	Clear
1000	Clear	Clear	Clear	Clear	Clear	Clear
10000	Clear	Clear	Clear	Clear	Clear	Clear
50000	Clear	Clear	Clear	Clear	Clear	Clear

Table A-3.45 10 000 ppm of Ca²⁺ and 30 000 ppm of NaCl for BHMTMPMA-O (pH 2).

Dose (ppm)	Appearance					
	At mixing	30 min	1 h	2 h	4 h	24 h
100	Clear	Clear	Clear	Clear	Clear	Clear
1000	Clear	Clear	Clear	Clear	Clear	Clear
10000	Clear	Clear	Clear	Clear	Clear	Clear
50000	Clear	Clear	Clear	Clear	Clear	Clear

BHMTMPMA (pH 6)

Table A-3.46 100 ppm of Ca²⁺ and 30 000 ppm of NaCl for BHMTMPMA (pH 6).

Dose (ppm)	Appearance					
	At mixing	30 min	1 h	2 h	4 h	24 h
100	Clear	Clear	Clear	Clear	Clear	Clear
1000	Clear	Clear	Clear	Clear	Clear	Clear
10000	Clear	Clear	Clear	Clear	Clear	Clear
50000	Clear	Clear	Clear	Clear	Clear	Clear

Table A-3.47 1 000 ppm of Ca²⁺ and 30 000 ppm of NaCl for BHMTMPMA (pH 6).

Dose (ppm)	Appearance					
	At mixing	30 min	1 h	2 h	4 h	24 h
100	Clear	Clear	Clear	Clear	Clear	Clear
1000	Clear	Clear	Clear	Clear	Clear	Clear
10000	Clear	Haze	Haze	Precipitated	Precipitated	Precipitated
50000	Clear	Clear	Clear	Clear	Clear	Clear

Table A-3.48 10 000 ppm of Ca²⁺ and 30 000 ppm of NaCl for BHMTMPMA (pH 6).

Dose (ppm)	Appearance					
	At mixing	30 min	1 h	2 h	4 h	24 h
100	Clear	Clear	Clear	Clear	Clear	Clear
1000	Clear	Slight haze	Slight haze	Slight haze/ precipitation	Haze/ precipitation	Haze/ precipitation
10000	Haze/ precipitated	Haze/ precipitated	Haze/ precipitated	Precipitated	Precipitated	Very precipitated
50000	Precipitated	Very precipitated	Very precipitated	Very precipitated	Very precipitated	Very precipitated

BHMTMPMA-O (pH 6)

Table A-3.49 100 ppm of Ca²⁺ and 30 000 ppm of NaCl for BHMTMPMA-O (pH 6).

Dose (ppm)	Appearance					
	At mixing	30 min	1 h	2 h	4 h	24 h
100	Clear	Clear	Clear	Clear	Clear	Clear
1000	Clear	Clear	Clear	Clear	Clear	Clear
10000	Clear	Clear	Clear	Clear	Clear	Clear
50000	Clear	Clear	Clear	Clear	Clear	Clear

Table A-3.50 1 000 ppm of Ca²⁺ and 30 000 ppm of NaCl for BHMTMPMA-O (pH 6).

Dose (ppm)	Appearance					
	At mixing	30 min	1 h	2 h	4 h	24 h
100	Clear	Clear	Clear	Clear	Clear	Clear
1000	Clear	Clear	Clear	Clear	Clear	Clear
10000	Clear	Haze	Haze	Haze	Haze/precipitated	Haze/precipitated
50000	Clear	Clear	Clear	Clear	Clear	Very slight precipitation

Table A-3.51 10 000 ppm of Ca²⁺ and 30 000 ppm of NaCl for BHMTMPMA-O (pH 6).

Dose (ppm)	Appearance					
	At mixing	30 min	1 h	2 h	4 h	24 h
100	Clear	Clear	Clear	Clear	Clear	Clear
1000	Clear	Very slight haze	Very slight haze	Very slight haze	Very slight haze	Very slight haze
10000	Haze	Haze/precipitated	Precipitated	Precipitated	Precipitated	Precipitated
50000	Precipitated	Clumpy precipitated	Clumpy precipitated	Clumpy precipitated	Clumpy precipitated	Clumpy precipitated